

## Original Article

**Cite this article:** Galloway JM, Vickers ML, Price GD, Poulton T, Grasby SE, Hadlari T, Beauchamp B, and Sulphur K (2020) Finding the VOICE: organic carbon isotope chemostratigraphy of Late Jurassic – Early Cretaceous Arctic Canada. *Geological Magazine* 157: 1643–1657. <https://doi.org/10.1017/S0016756819001316>

Received: 4 April 2019

Revised: 6 September 2019

Accepted: 7 October 2019

First published online: 20 December 2019

**Keywords:**

Arctic; Jurassic–Cretaceous; Canada; carbon isotopes



**Author for correspondence:**

Jennifer M. Galloway,

Emails: [Jennifer.Galloway@aias.au.dk](mailto:Jennifer.Galloway@aias.au.dk);

[Jennifer.Galloway@canada.ca](mailto:Jennifer.Galloway@canada.ca)

# Finding the VOICE: organic carbon isotope chemostratigraphy of Late Jurassic – Early Cretaceous Arctic Canada

Jennifer M. Galloway<sup>1,2</sup> , Madeleine L. Vickers<sup>3</sup>, Gregory D. Price<sup>4</sup>, Terence Poulton<sup>1</sup>, Stephen E. Grasby<sup>1</sup>, Thomas Hadlari<sup>1</sup> , Benoit Beauchamp<sup>5</sup> and Kyle Sulphur<sup>1,5</sup>

<sup>1</sup>Geological Survey of Canada/Commission géologique du Canada, Natural Resources Canada/Ressources naturelles Canada, 3303 33rd St N.W., Calgary, Alberta T2L 2A7, Canada; <sup>2</sup>Aarhus Institute of Advanced Studies, Aarhus University, Høegh-Guldbergs Gade 6B 8000 Aarhus C, Denmark; <sup>3</sup>Faculty of Science, Geology Section, University of Copenhagen, Øster Voldgade 10, DK-1350 Copenhagen K, Denmark; <sup>4</sup>School of Geography, Earth & Environmental Sciences, University of Plymouth, Drake Circus, PL4 8AA, UK and <sup>5</sup>Department of Geosciences, University of Calgary, Calgary, AB T2N 1N4, Canada

**Abstract**

A new carbon isotope record for two high-latitude sedimentary successions that span the Jurassic–Cretaceous boundary interval in the Sverdrup Basin of Arctic Canada is presented. This study, combined with other published Arctic data, shows a large negative isotopic excursion of organic carbon ( $\delta^{13}\text{C}_{\text{org}}$ ) of 4‰ (V-PDB) and to a minimum of  $-30.7\text{‰}$  in the probable middle Volgian Stage. This is followed by a return to less negative values of  $c. -27\text{‰}$ . A smaller positive excursion in the Valanginian Stage of  $c. 2\text{‰}$ , reaching maximum values of  $-24.6\text{‰}$ , is related to the Weissert Event. The Volgian isotopic trends are consistent with other high-latitude records but do not appear in  $\delta^{13}\text{C}_{\text{carb}}$  records of Tethyan Tithonian strata. In the absence of any obvious definitive cause for the depleted  $\delta^{13}\text{C}_{\text{org}}$  anomaly, we suggest several possible contributing factors. The Sverdrup Basin and other Arctic areas may have experienced compositional evolution away from open-marine  $\delta^{13}\text{C}$  values during the Volgian Age due to low global or large-scale regional sea levels, and later become effectively coupled to global oceans by Valanginian time when sea level rose. A geologically sudden increase in volcanism may have caused the large negative  $\delta^{13}\text{C}_{\text{org}}$  values seen in the Arctic Volgian records but the lack of precise geochronological age control for the Jurassic–Cretaceous boundary precludes direct comparison with potentially coincident events, such as the Shatsky Rise. This study offers improved correlation constraints and a refined C-isotope curve for the Boreal region throughout latest Jurassic and earliest Cretaceous time.

**1. Introduction**

The Jurassic–Cretaceous boundary interval was characterized by significant fluctuations in Earth system processes (Hallam, 1986; Ogg & Lowrie, 1986; Sager *et al.* 2013; Price *et al.* 2016) that resulted in the extinction of many marine invertebrates (Hallam, 1986; Alroy, 2010; Tennant *et al.* 2017). Despite its importance in Earth history, the precise radiometric age and correlations of the Jurassic–Cretaceous boundary interval are poorly understood compared with those of other Phanerozoic environmental crises. This is partly because of the previous lack of a robust, global chronostratigraphic framework for the boundary (Zakharov *et al.* 1996; Wimbledon *et al.* 2011). After long debate, the Berriasian Working Group of the International Subcommission on Cretaceous Stratigraphy has voted to adopt the base of the *Calpionella alpina* Subzone as the primary marker for the base of the Berriasian Stage in the Tethyan faunal realm (Wimbledon, 2017). At this time, a stratotype section has not been formally designated. This potential Global Boundary Stratotype Section and Point (GSSP) level cannot be traced biostratigraphically into Arctic areas (e.g. Wimbledon, 2017, fig. 1). Palaeomagnetic reversal data may provide direct Boreal–Tethyan correlation for the Tithonian–Berriasian boundary eventually, but data from the Boreal Nordvik section (Houša *et al.* 2007; Bragin *et al.* 2013; Schnabl *et al.* 2015) remain to be confirmed in other Arctic sections. Alternative options for the placement of the Jurassic–Cretaceous boundary continue to find support.

Although the international chronostratigraphic terminology for the Jurassic–Cretaceous boundary interval (Tithonian and Berriasian stages) is increasingly being used in Canadian Arctic studies, interpretations of the correlations of the substages and fossil zones entailed in these Tethys-based stages into the Arctic vary among global workers. Particularly contentious and significant is how much of the upper Volgian Stage is time-equivalent with the lower Berriasian Stage. Our usage in this report of the roughly equivalent Boreal (Volgian, Ryazanian)

and Tethyan nomenclature follows that of the relevant original literature cited. Our data do not contribute to, or require, discussion of their detailed correlations or about the common but potentially misleading use of the term Boreal for some NW European Sub-boreal sequences.

The numerical age of the Jurassic–Cretaceous boundary is also under debate. The International Commission of Stratigraphy (Cohen *et al.* 2013, updated 2018/08) places the Jurassic–Cretaceous boundary at *c.* 145 Ma following Mahoney *et al.* (2005), who suggest a minimum age for the boundary based on mean  $^{40}\text{Ar}$ – $^{39}\text{Ar}$  ages of  $144.6 \pm 0.8$  Ma, although recent U–Pb studies by Aguirre-Urreta *et al.* (2019) and Lena *et al.* (2019) provide new U–Pb ages that suggest that the numerical age of the boundary is more likely as young as 140–141 Ma.

A small change to lower  $\delta^{13}\text{C}$  values occurs within Magnetozone M18–M17, and within the B/C Calpionellid Zone (Weissert & Channell, 1989), that contrast with more positive values obtained from the Valanginian Stage (Lini *et al.* 1992; Price *et al.* 2016). Such variation suggests that carbon isotope anomalies may be useful to characterize the Jurassic–Cretaceous boundary interval (e.g. Michalík *et al.* 2009; Dzyuba *et al.* 2013). A recent global stack compiled by Price *et al.* (2016) that included data from many sites spanning a range of mainly southerly latitudes, and was therefore considered representative of the global carbon isotopic signal, showed that the composite  $\delta^{13}\text{C}_{\text{carb}}$  curve from the base of the Kimmeridgian stage to the base of the Valanginian stage has no major perturbations. However, there is a paucity of published  $\delta^{13}\text{C}$  data from Arctic regions and, in those that do exist, there is notably greater variation in high-northern-latitude  $\delta^{13}\text{C}_{\text{org}}$  (e.g. Hammer *et al.* 2012) than in better-studied middle- to low-latitude carbonate records ( $\delta^{13}\text{C}_{\text{carb}}$ ) (Price *et al.* 2016) or in  $\delta^{13}\text{C}_{\text{carb}}$  records from belemnites in Arctic successions (Žák *et al.* 2011).

Hammer *et al.* (2012) present  $\delta^{13}\text{C}_{\text{org}}$  data for the Upper Jurassic – lowermost Cretaceous systems of central Spitsbergen. This record shows a middle Volgian excursion of *c.* 5‰ that they term the Volgian Isotopic Carbon Excursion (VOICE). Koevoets *et al.* (2016) documented a middle Volgian negative excursion in  $\delta^{13}\text{C}_{\text{org}}$  of *c.* 3‰ in the Agardhfjellet Formation of central Spitsbergen. Records from northern Siberia also document a  $\delta^{13}\text{C}_{\text{org}}$  excursion to isotopically lighter values in the upper middle Volgian (*Exoticus* Zone; Zakharov *et al.* 2014), but with no parallel trend in  $\delta^{13}\text{C}_{\text{carb}}$  measured in belemnite rostra from the same section (Žák *et al.* 2011); this is possibly because carbon isotopes preserved in belemnite rostra may not be in equilibrium with ambient seawater (Wierzbowski & Joachimski, 2009). Turner *et al.* (2019) report a  $\delta^{13}\text{C}_{\text{org}}$  curve from the 6406/12-2 drill core from the Norwegian Sea that spans the interval from the base of the *Pallasioides* Zone to the top of the *Rotunda* Zone. A negative isotopic excursion occurs in the *Pallasioides* Zone that the authors relate to VOICE. Further south, Morgans-Bell *et al.* (2001) examined the carbon isotope stratigraphy of organic matter preserved in the Wessex Basin. Their record extends into the Upper Jurassic System but does not continue through to the lowest Berriasian Stage. This curve shows a trend of declining  $\delta^{13}\text{C}_{\text{org}}$  of much greater magnitude than the time-equivalent carbonate curve.

Alternative correlation tools, such as geochemical anomalies in marine strata, may therefore aid with future correlations of Jurassic–Cretaceous strata, particularly in high northern latitudes. A new  $\delta^{13}\text{C}_{\text{org}}$  record from Upper Jurassic – Lower Cretaceous argillaceous strata from two stratigraphic sections

in the Sverdrup Basin, Arctic Canada, is presented here. Geochemical trends are compared with data from other high-latitude successions as well as with Tethyan sections to evaluate their palaeoceanographic and palaeoclimatic importance and potential for stratigraphic correlation. In the absence of any obvious definitive cause for VOICE, several possible contributing factors, both regional and distant, are considered and discussed.

## 2. Study area

The Sverdrup Basin is a  $1300 \times 350$  km palaeo-depocentre in the Canadian Arctic Archipelago that contains up to 13 km of nearly continuous Carboniferous–Palaeogene strata (Figs 1, 2; Balkwill, 1978; Embry & Beauchamp, 2019).

Basin subsidence began following rift collapse of the Ellesmerian Orogenic Belt during early Carboniferous time (Embry & Beauchamp, 2019). Rifting of the Sverdrup Basin continued during the late Carboniferous Period and led to widespread flooding of the rift basin and increasingly open-marine connections with Panthalassa and North Greenland and the Barents Sea (Embry & Beauchamp, 2019). After the first rift phase, marine deposition persisted through the Permian and Triassic periods. A second phase of rifting began in the Early Jurassic, continued through the Late Jurassic – earliest Cretaceous interval, and then ceased in the Sverdrup Basin when seafloor spreading began in the adjacent proto-Amerasia Basin to form the Arctic Ocean (Hadlari *et al.* 2016). Deposition in the Sverdrup Basin ended in the Palaeogene Period due to regional compression and widespread uplift associated with the Eureka Orogeny (Embry & Beauchamp, 2019).

In the Late Jurassic, the Sverdrup Basin was one of many rift basins that formed during the break-up of Pangea and affected palaeoceanographic connections between the western Tethys and Panthalassa in northern latitudes. Deposition of the Deer Bay Formation during latest Jurassic – earliest Cretaceous time marked a rift climax in the Sverdrup Basin prior to the break-up of the adjacent proto-Amerasia Basin, manifested as a sub-Hauterivian break-up unconformity in the Sverdrup Basin (Galloway *et al.* 2013; Hadlari *et al.* 2016; Fig. 2). The Deer Bay Formation is therefore a lithostratigraphic unit of interest from both a tectonostratigraphic and palaeoceanographic perspective; its study may provide insight into both regional and global changes at this dynamic time in Earth's history.

The Deer Bay Formation is a succession of mudstone with interbeds of siltstone and very-fine-grained sandstone deposited in pro-delta to offshore shelf environments across the Sverdrup Basin during the Volgian to Valanginian ages (Heywood, 1957; Balkwill, 1983; Embry, 1985). The Deer Bay Formation reaches a maximum thickness of 1375 m on eastern Ellef Ringnes Island and 920 m on Axel Heiberg Island (Balkwill, 1983). Offshore shelf mudstones of the Deer Bay Formation conformably overlie either the shallow-shelf sandstones of the Awingak Formation or the Ringnes Formation, its offshore-shelf mudstone equivalent (Fig. 2). Deer Bay mudstones grade conformably into delta-front and fluvial-deltaic sands of the overlying Isachsen Formation along the axis of Sverdrup Basin (Fig. 2; Balkwill, 1983; Embry, 1985), but these formational contacts are disconformable on basin margins (Hadlari *et al.* 2016; Embry & Beauchamp, 2019). The Deer Bay Formation is undivided except for the designation of the *c.* 40 m sandstone-dominated Glacier Fiord Member in its upper part on southern Axel Heiberg Island, south of the study area

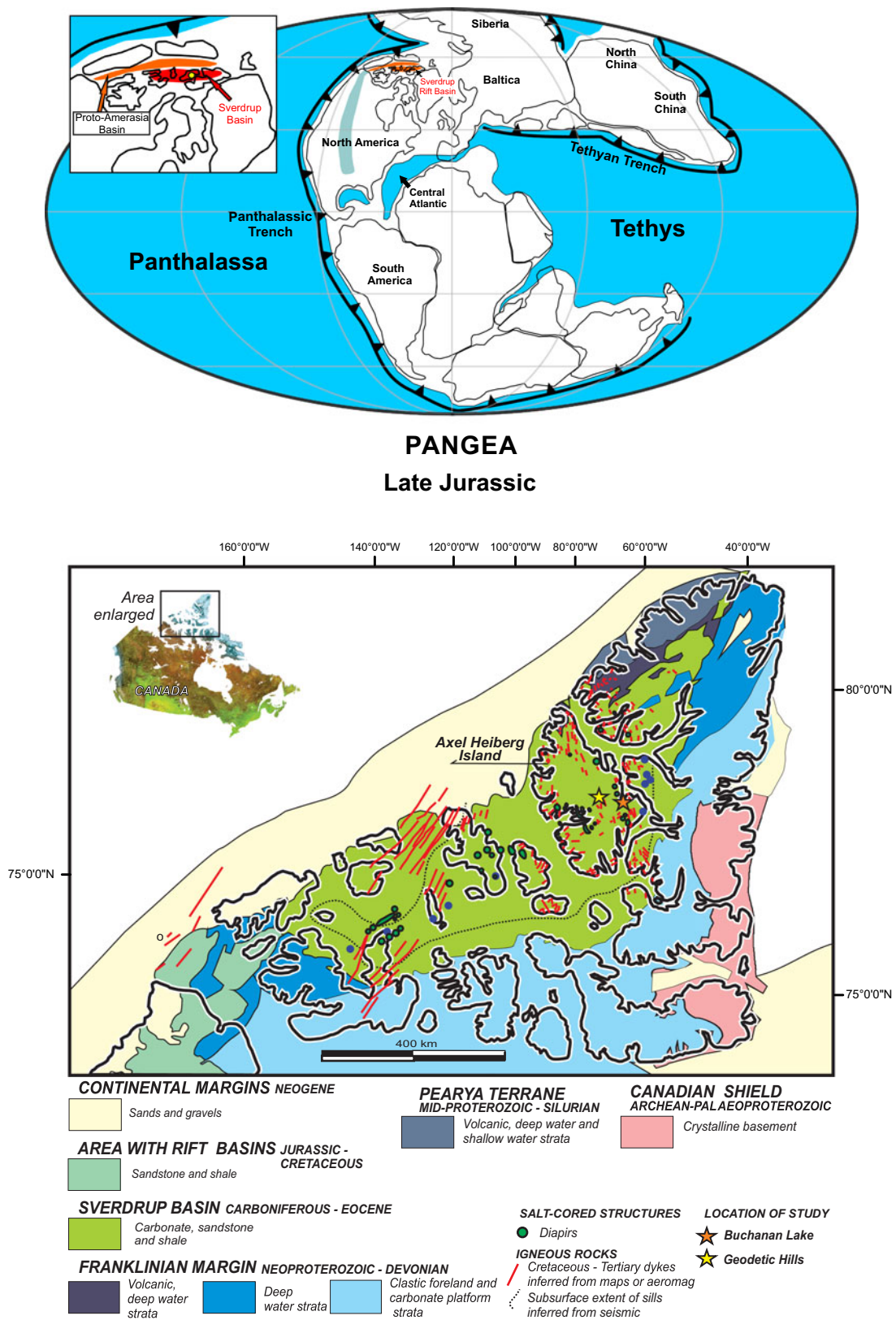


**Fig. 1.** Upper: palaeogeographic map of Pangea at c. 150 Ma (Tithonian; modified from Scotese, 2014), with modifications from Amato *et al.* (2015), Midwinter *et al.* (2016) and Hadlari *et al.* (2016, 2017, 2018). Arc and microcontinental terranes that had not yet docked with the North American and Siberian accretionary margins are not illustrated in the palaeo-Pacific Ocean (Panthalassa). Lower: map of the Sverdrup Basin showing location of stratigraphic sections studied at Geodetic Hills and Buchanan Lake, Axel Heiberg Island, Nunavut. After Dewing *et al.* (2007).

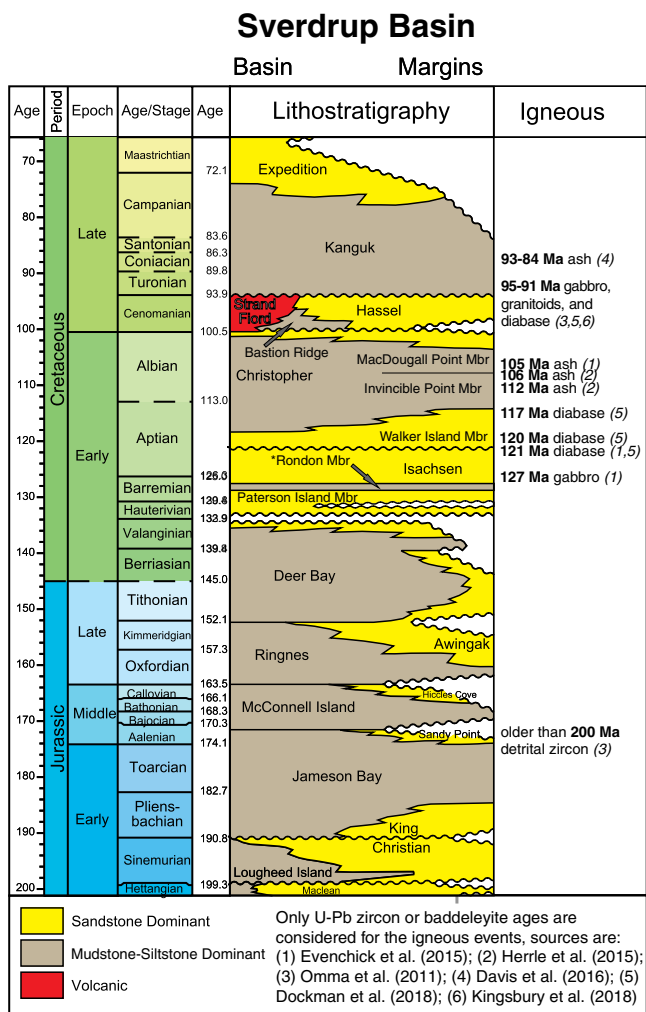


**Fig. 2.** Mesozoic lithostratigraphy of Sverdrup Basin (after Hadlari *et al.* 2016). The International Chronostratigraphic Chart (ICS) v 2018/08 (Cohen *et al.* 2013; updated) is used for absolute ages. Note that intrusive ages should be younger than the intruded strata, and that detrital zircon ages can be older.

(Embry, 1985). In other localities, this member is absent from shale facies or because of truncation below an intra- or sub-Isachsen unconformity (Embry, 1985). Concretions of various compositions, size and shape occur throughout the Deer Bay Formation, with large (up to 5 m long) calcitic and sideritic mudstone concretions common in its lower portion. Glendonites occur in multiple horizons that range in thickness from 2 to 20 m throughout the Deer Bay Formation and are most common in its upper Valanginian portion (Kemper, 1975, 1983, 1987; Kemper & Jeletzky, 1979; Selmeier & Grosser, 2011; Grasby *et al.* 2017). This upper interval is further characterized by finely laminated siltstones and fissile shales that host rare thin rusty-weathering calcareous layers and irregularly distributed intervals of calcareous concretions (Heywood, 1957; Kemper, 1975; Balkwill, 1983). The biostratigraphic framework of the glendonite-bearing Valanginian succession was described by Kemper (1975, 1977, 1987) based on ammonites in successions exposed on Amund Ringnes (lower Valanginian) and Ellef Ringnes (upper Valanginian) islands. These strata also contain age-diagnostic marine bivalves, including *Buchia keyserlingi* (Lahusen) and belemnites (Jeletzky, 1973; Kemper, 1977).

### 3. Materials and methods

A total of 154 samples were collected every c. 1.5–2 m throughout a 255 m exposure of the Deer Bay Formation at Buchanan Lake (79° 22' 0.47" N, 87° 46' 9.03" W), and 92 samples were collected every c. 3–4 m from a 388 m exposure of the Deer Bay Formation at Geodetics Hills (79° 48' 57.20" N, 89° 48' 20.41" W), Axel Heiberg Island (Fig. 1). Bivalves, belemnites and ammonites were collected from the Buchanan Lake section; macrofossils were not observed at the Geodetic Hills section. All samples are stored in permanent collections of the Geological Survey of Canada.

Mudstone samples were pre-treated with 10% HCl to remove carbonates, and then  $\delta^{13}\text{C}$  analysis of organic carbon was performed using a Elemental VarioEL Cube Elemental Analyser followed by a trap-and-purge separation and online analysis by continuous flow with a DeltaPlus Advantage isotope ratio mass spectrometer coupled with a ConFlo III interface at the GG Hatch Stable Isotope Laboratory, University of Ottawa. Results are reported as ‰ relative to Vienna Pee Dee belemnite (V-PDB) and normalized to international standards calibrated to the international standards IAEA-CH-6 (−10.4‰), NBS-22 (−29.91‰), USGS-40 (−26.24‰) and USGS-41 (37.76‰). Long-term analytical precision is based on blind analysis of the internal standard C-55 (glutamine; −28.53‰) not used for calibration, and is routinely better than 0.2‰. For the Buchanan Lake dataset ( $n = 154$ ), 14 quality control duplicate analyses were run (representing 9% of the samples). For the Geodetic Hills dataset ( $n = 92$ ), 12 quality control duplicate analyses were run (12%) (online Supplementary Material available at <http://journals.cambridge.org/geo>). Average relative percent difference (RPD) was  $0.13 \pm 0.10\%$  SD ( $n = 14$ ) for the Buchanan Lake samples and  $0.55 \pm 0.42\%$  SD ( $n = 12$ ) for the Geodetic Hills material. The blind standard C-55 was run in triplicate for each of the three batches to assess accuracy. The average RPD between the measured and expected value of the standard was  $0.18 \pm 0.13\%$  SD ( $n = 9$ ).

Organic carbon isotopic composition can be influenced by the type and maturity of organic matter; Rock-Eval pyrolysis was therefore conducted on all samples. Total organic carbon (TOC, wt%) was determined by Rock-Eval 6 (Vinci Technologies, France) pyrolysis as the sum of organic matter during pyrolysis (pyrolysable carbon, 100–650°C) and oxidation (residual carbon, 400–850°C) on all samples. Analyses of standard reference materials (IFP 160000, Institut Français du Pétrole; internal 9107 shale standard, Geological Survey of Canada, Calgary; Ardakani *et al.* 2016) was run every fifth sample demonstrating a < 1% relative standard deviation (RSD) for TOC, < 3% RSD for S1 and S2, and 11% RSD for S3. The lower accuracy for S3 in bulk samples was expected due to poor peak integration and distinction between S3 organic matter and S3 carbonates that may occur because of the presence of siderite in standards (Ardakani *et al.* 2016). Duplicate analyses were conducted for assessment of analytical precision. In the Buchanan Lake dataset 22 duplicate samples were run, and in the Geodetic Hills dataset two duplicate samples were run (online Supplementary Material available at <http://journals.cambridge.org/geo>). Samples from both sections comprised the analytical batch from which quality control duplicate samples were randomly selected. Average RPD for TOC (wt%) was  $16.75 \pm 26.93$ , S1 is  $13.21 \pm 15.34$ , S2 is  $9.56 \pm 13.67$  and S3 is  $11.02 \pm 14.30$  ( $n = 24$ ).

### 4. Results

#### 4.a. Macrofossils and age of strata

Macrofossils were found during this study in the middle and upper parts of the Deer Bay Formation in the Buchanan Lake section and

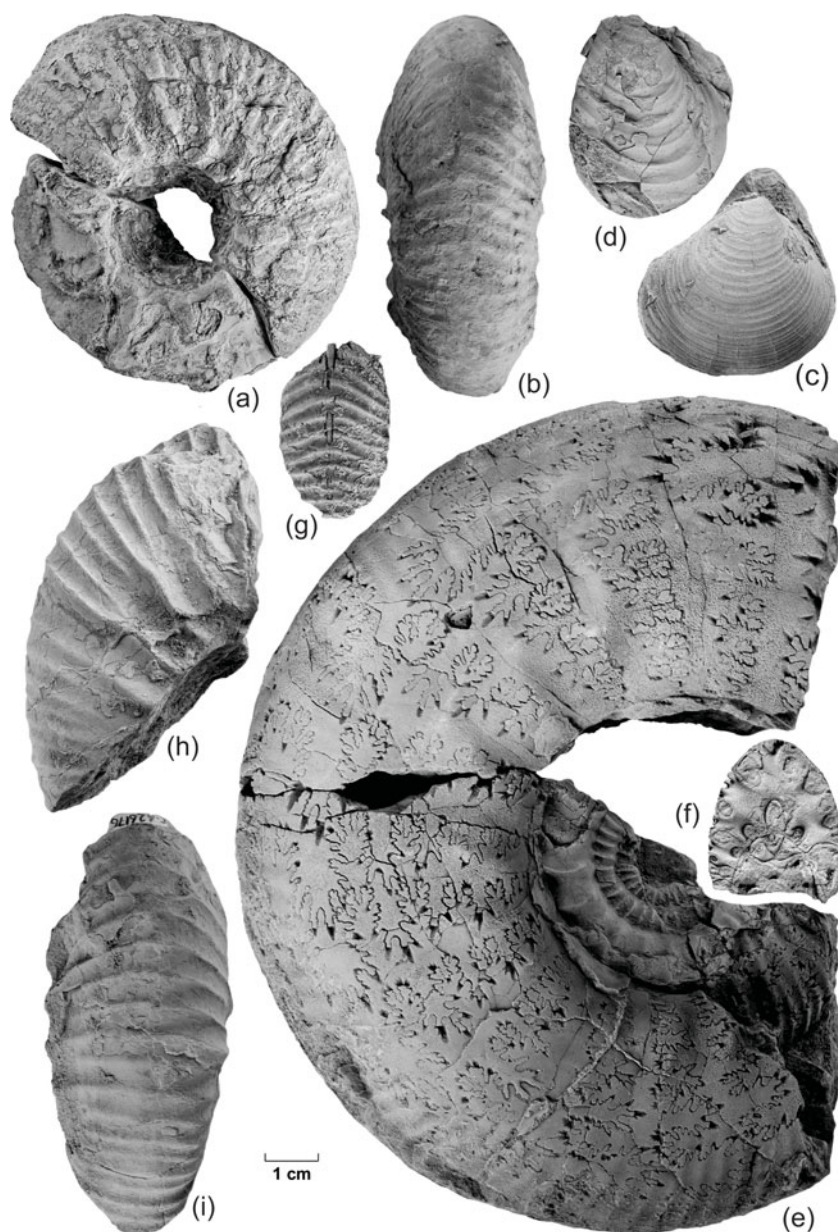


**Fig. 3.** All fossils are stored in the National Type Invertebrate Collection of the Geological Survey of Canada. The size of all figures can be judged by the 1 cm scale bar, except (f) which is half the scale of the others and of the scale bar. (a, b) *Nikitinoceras kemperi* (Jeletzky). GSC 140515 (figured specimen number) from GSC locality C-626163 (GSC curation number), lateral and ventral views. (c) *Buchia* sp. cf. *inflata* (Toula). GSC 140516 from GSC locality C-626163. (d) *Buchia okensis* (Pavlov). GSC 140517 from GSC locality C-626165. (e–g) *Borealites* (*Pseudocraspedites*) sp. (e, f) GSC 140518 from GSC locality C-626176, macroconch phragmocone fragment, lateral view and cross-section (at adoral preserved end; size reduced  $\times 1/2$ ) views of septate inner cast; and (g) ventral view of part of inner whorl. Another larger phragmocone fragment, with outer shell surface, is septate to a whorl height of at least 7 cm. (h, i) *Borealites* sp. GSC 140519 from GSC locality C-626176, lateral and ventral views, outer shell surface.

were not seen in the Geodetic Hills section. The Buchanan Lake macrofossils are, from top of the section to the base: (1) small impressions of *Buchia* sp., 76 m below the base of the Isachsen Formation (GSC loc. C-626162); age, undeterminable within the late Oxfordian – Valanginian interval; (2) several fragments of ammonite *Nikitinoceras kemperi* (Jeletzky) (Fig. 3a, b), bivalve *Buchia* sp. cf. *inflata* (Toula) (Fig. 3c) and belemnites *Acroteuthis?* and *Cylindroteuthis?* (C-626163) occur 75.5 m below the base of the Isachsen Formation; age, early Valanginian; (3) numerous impressions of *Buchia okensis* (Pavlov) or *B.* sp. aff. *okensis* (*sensu* Jeletzky 1964, 1984) occur 77 m below the base of the Isachsen Formation (C-626165; Fig. 3d); age, early Ryazanian (i.e. Berriasian, but probably not earliest Berriasian equivalent); (4) fragments of bivalves 125 m below the base of the Isachsen Formation including *Buchia* sp. aff. *okensis*, *Mclearnia?*, *Oxytoma?* and *Meleagrinnella?*, with unidentified gastropods and the belemnite *Acroteuthis* (C-626172); of probable early Ryazanian age; and (5) several fragments of relatively large *Borealites* (*Pseudocraspedites*) (Fig. 3e–g) and of *Borealites* s.l. (Fig. 3h, i) occur 143 m below

the Isachsen Formation (C-626176) and are of early Ryazanian age. Poorly preserved, unidentifiable fossil fragments occur in still lower beds and above the carbon isotope anomaly. Mikhail Rogov (pers. comm., 2019) has assisted us with our identification of the specimens we have assigned to *Nikitinoceras* and *Borealites*.

The *Borealites* specimens are the lowest in our collections and provide a youngest age limit for the lower negative  $\delta^{13}\text{C}$  anomaly at Buchanan Lake. A previous fossil collection from perhaps the same level as our *Borealites* fauna and in a similarly prolific horizon (GSC loc. 26171, 316 feet = 96.3 m above the base of the Deer Bay Formation according to Souther, 1963, p. 438) contains ammonites closely similar to ours. They were initially reported as Valanginian (Friebold, in Souther, 1963) but were figured, together with associated *Buchia okensis*, as lower Berriasian *Tollia* (*Subcraspedites*) aff. *suprasubditus* (Bogoslovsky) by Jeletzky (1964, plate I–III), as *Craspedites* (*Subcraspedites*) by Jeletzky (1973, plate 6, from “136.6–140 metres above base” of the formation, which we take to be mistaken) and as *Tollia* (*Subcraspedites*) aff. *suprasubditus* by

Jeletzky (1984, p. 223, at the “95 m level”). Jeletzky (1973, 1984) also reported similar faunas at higher levels, but acknowledged confusion about their stratigraphic levels and noted re-assignment of the ammonites to *Praetollia* (*Pseudocraspedites*) and *P.* (*Praetollia*), now included in *Borealites* (Wright et al. 1996), and thought *Craspedites* (*Taimyroceras?*) *canadensis* Jeletzky to occur below them.

We did not find fossils to control the older age limit for the negative  $\delta^{13}\text{C}$  anomaly in the sections studied. However, Jeletzky (1984, p. 221, GSC loc. 26156) reported generically indeterminate dorsoplanitid ammonites and large *Buchia fischeriana* (d’Orbigny) from “an 8 m bed commencing 31 m” above the base of the Deer Bay Formation along the Awingak River, that is, near or within our Buchanan Lake section. The collection has not been relocated but, if the fossils are correctly determined, they imply a middle, perhaps early middle, Volgian age for this interval, which would fall at about the maximum depletion point of the  $\delta^{13}\text{C}$  curve. Dorsoplanitid ammonites and various associated *Buchia* species including *B. fischeriana* (d’Orbigny) are widespread on nearby Ellesmere Island (Jeletzky, 1984; Schneider et al. 2019) and indicate a middle Volgian age for the lower Deer Bay Formation and its initial transgression event throughout eastern Sverdrup Basin. Jeletzky (1984, p. 223) also reported other unidentifiable ammonites and bivalves in lower parts of the Buchanan Lake succession. Two reports of *Buchia mosquensis* (von Buch) from Amund Ringnes Island (Jeletzky, in Balkwill et al. 1977, p. 1136) may be early Volgian, rare indicators of this interval in the more axial portion of the basin, or they may be late Kimmeridgian in age.

Stratigraphically close juxtaposition of early Ryazanian and early Valanginian fossils supports the interpretation of a strongly condensed interval or basinal disconformity at the Buchanan Lake locality near the depocentre of the Sverdrup Basin. The apparent absence of diagnostic fossils of late Berriasian age across the Sverdrup Basin has been used previously to suggest a widespread sub-Valanginian disconformity (Jeletzky, 1973; Kemper, 1975; Embry, 2011).

The Valanginian strata in the northern and eastern parts of Sverdrup Basin, as across the Arctic, are replete with glendonites (Kemper & Schmitz, 1975; Grasby et al. 2017; Rogov et al. 2017), but minor occurrences of ‘stellate nodules’ or ‘carbonate crystal rosettes’ have been reported in upper Oxfordian or lower Kimmeridgian strata to Berriasian strata in the western Sverdrup Basin (Poulton, 1994, p. 183), northern Yukon (Poulton, 1996, p. 285), and the Northwest Territories (Mountjoy & Procter, 1969). While their appearance in only the upper 104 m of the Buchanan Lake section of the Deer Bay Formation at Buchanan Lake might suggest pre-Valanginian ages for the underlying strata, the interval with glendonites overlap with strata containing *Buchia okensis*, or *B.* cf. and aff. *okensis*, collected in this study and reported by Jeletzky (1984, p. 221, 223). They may indicate an age for the associated glendonites as old as early Ryazanian, although it is possible that they developed within the lower Ryazanian strata exposed on the sea floor during Valanginian time.

#### 4.b. Carbon isotopes

Measured  $\delta^{13}\text{C}_{\text{org}}$  values fall within a range of  $-30.7$  to  $-24.6\text{‰}$  (V-PDB) for both sections ( $n = 92$  Geodetic Hills section;  $n = 154$  Buchanan Lake section; see online Supplementary Material available at <http://journals.cambridge.org/geo>). Two outliers (A124, A21) in the Buchanan Lake dataset were removed. Without further evidence, we disregard these values as outliers due to contamination. A negative  $\delta^{13}\text{C}_{\text{org}}$  excursion, with a magnitude of  $c. 4\text{‰}$  and reaching minimum values of  $-29.8\text{‰}$  at Buchanan Lake and

$-30.7\text{‰}$  at Geodetic Hills, is observed within the lower Deer Bay Formation. All of the recovered macrofossils from the Buchanan Lake section occur stratigraphically above the negative carbon isotope excursion, dating the overlying strata as late Volgian or Ryazanian in age and younger in the Buchanan Lake section. This negative  $\delta^{13}\text{C}_{\text{org}}$  excursion is followed by a return to less negative values of  $c. -27\text{‰}$ . A small negative shift of  $c. 1.5\text{‰}$  occurs in strata that are likely late middle Volgian or early late Volgian in age, and this is followed by an interval of generally increasing values across the interpreted Jurassic–Cretaceous boundary until the upper Valanginian part of the Deer Bay Formation. A positive carbon isotope excursion is evident in its upper part in both sections, with a magnitude of  $c. 1.5\text{‰}$  (interpreted here as the Weissert Event; Erba et al. 2004). Carbon-13 isotope ratios reach maximum values of  $-24.6\text{‰}$  at Buchanan Lake and  $-24.9\text{‰}$  at Geodetic Hills during this event (Fig. 4).

#### 4.c. Rock-Eval 6 pyrolysis

TOC measured by Rock-Eval 6 pyrolysis on samples of the Buchanan Lake section (median TOC 1.16 wt%; range 0.09–4.36 wt%;  $n = 154$ ) and Geodetic Hills section (median TOC 1.48 wt%; range 0.48–5.87 wt%,  $n = 92$ ) are typical for high-latitude Upper Jurassic and Lower Cretaceous mudrock successions (cf. Hammer et al. 2011). The TOC range indicates poor to excellent source rock (see online Supplementary Material available at <http://journals.cambridge.org/geo>). Thermal alteration of material indicated by  $T_{\text{max}}$  (the temperature corresponding to maximum S2 during pyrolysis) ranges from 427 to 499°C in samples collected from the Buchanan Lake section and from 436 to 448°C in samples collected from the Geodetic Hills section; the majority of samples from both sections are in the oil window. The S2 values (amount of hydrocarbons generated by thermal cracking of organic matter) and S3 (the amount of  $\text{CO}_2$  released during thermal breakdown of kerogen) range from 0.15 to 2.42 mg HC/g and 0.27–2.41 mg HC/g at Buchanan Lake, respectively ( $n = 154$ ). S2 and S3 range from 0.22 to 6.13 mg HC/g TOC and 0.13–1.27 mg HG/g TOC, respectively, at Geodetic Hills ( $n = 92$ ). The hydrogen index (HI = S2/g TOC) and oxygen index (OI = S3/g TOC) suggest that organic matter is predominantly Type III kerogen at Buchanan Lake and a mixture of Type II and III kerogen in the Geodetic Hills samples (Fig. 5). The Geodetic Hills locality was more distal and in a deeper part of the basin during latest Jurassic – earliest Cretaceous times than the Buchanan Lake locality, and this is reflected in the higher proportion of Type III kerogen at Buchanan Lake. Samples with very low TOC resulted in HI or OI values  $> 200$  (Buchanan Lake A22, A43, A56, A65, A76, A82, A121 and A124) and are not plotted on the Van Krevelen diagram (Fig. 5) or stratigraphically (Fig. 6). Stratigraphic trends in TOC, HI and OI are shown in Figure 6. In both the Buchanan Lake and Geodetic Hills sections, TOC increases near the top of the Deer Bay Formation. Trends in HI and OI are also similar between the two sections, with marginally higher HI values near the base of the Deer Bay Formation.

Spearman’s rank correlation was conducted to evaluate relationships between  $\delta^{13}\text{C}_{\text{org}}$  and organic matter source and maturity. In both sections,  $\delta^{13}\text{C}_{\text{org}}$  is significantly related to TOC (Buchanan Lake  $\delta^{13}\text{C}_{\text{org}}$ :TOC  $r_s = 0.3$ ,  $P < 0.001$ ,  $n = 146$  with outliers A22, A43, A56, A65, A76, A82, A121 and A124 removed; Geodetic Hills  $\delta^{13}\text{C}_{\text{org}}$ :TOC  $r_s = 0.43$ ,  $P < 0.001$ ,  $n = 92$ ). In the Buchanan Lake samples,  $\delta^{13}\text{C}_{\text{org}}$  is also significantly ( $P < 0.001$ ) correlated with S1 ( $r_s = -0.34$ ), S3 ( $r_s = 0.33$ ) and HI ( $r_s = -0.3$ ), but these

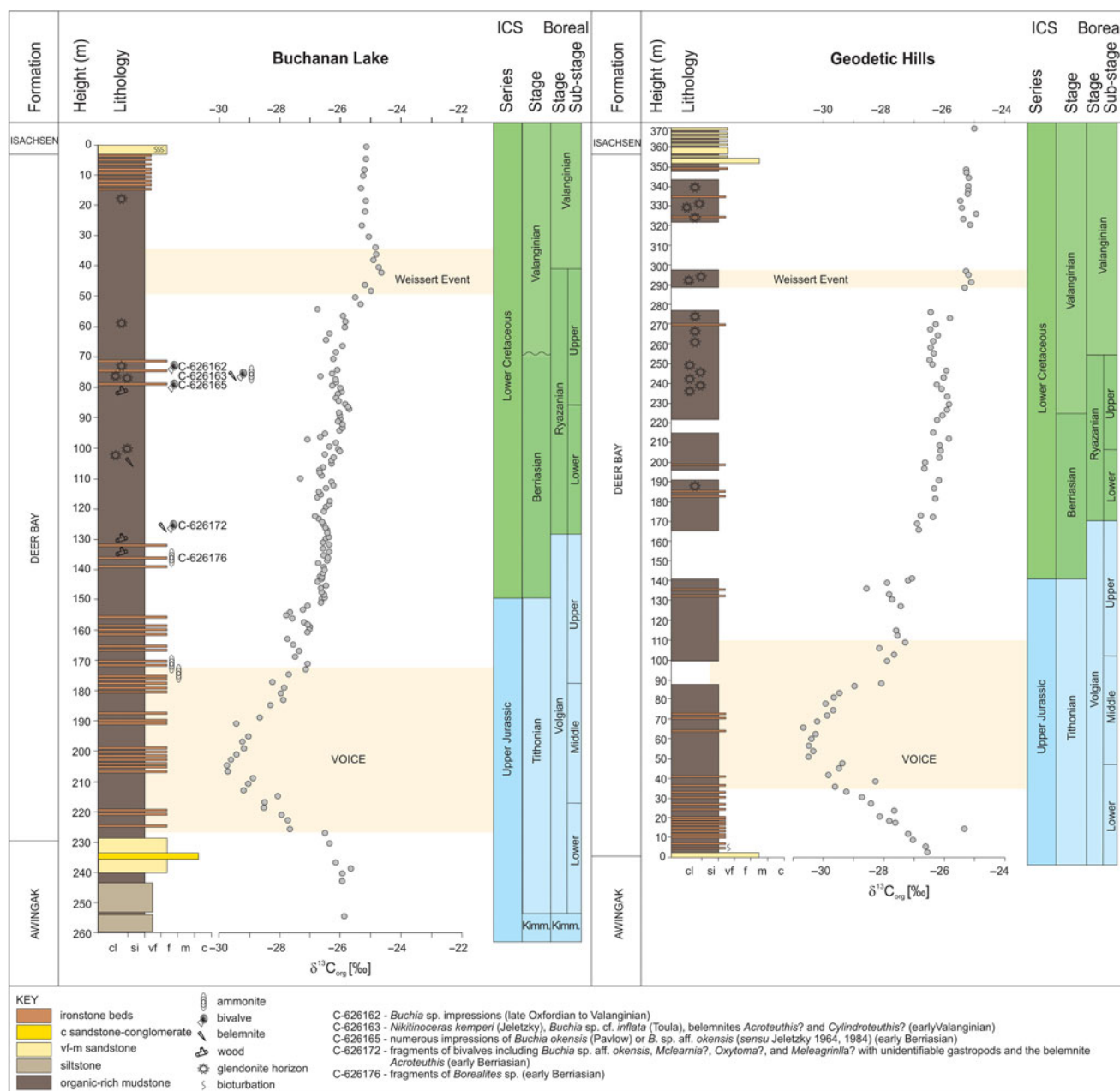


**Fig. 4.** Buchanan Lake and Geodetic Hills stratigraphy and  $\delta^{13}C_{org}$ . The datum for measurement of the Buchanan Lake section was the Isachsen – Deer Bay formational contact; the datum for measurement of the Geodetic Hills section was the Awingak – Deer Bay formation contact. The International Chronostratigraphic Chart (ICS) v 2018/08 (Cohen *et al.* 2013; updated) and Boreal Stage and Sub-stage (after Shurygin & Dzyuba *et al.* 2015) are shown.

relationships are insignificant in the Geodetic Hills samples. In both sections the relationships between  $\delta^{13}C_{org}$ ,  $T_{max}$  and S2 are insignificant ( $P > 0.05$ ). While statistically significant, the relationships between  $\delta^{13}C_{org}$  and organic matter parameters (TOC in both sections, S1 and S3 for Buchanan Lake) are weak as shown by the low values of  $r_s$ , suggesting that the influence of organic matter source, diagenesis and thermal maturation on the  $\delta^{13}C_{org}$  values is limited. The high thermal maturity ( $T_{max}$ , 427–499°C Buchanan Lake and 436–448°C in Geodetic Hills) of the material could complicate interpretations of the Rock Eval pyrolysis data. Thermal degradation may disguise a change in organic matter source as heating pushes kerogen types to low HI (Hunt, 1996). Degraded, oxidized, residual ‘dry-gas-type’ kerogen (Type IV) falls into the same category as Type III on a van Krevelen-type plot (Tyson, 1995); a

change in organic matter source from dominantly terrestrial (Type III) to marine (Type II) may therefore not be recognizable in an HI-OI cross-plot/van Krevelen-type diagram if the organic matter became highly thermally degraded. However, the reproduction of the carbon isotope curve in two stratigraphic sections, and consistency with curves from other Arctic areas, lends confidence to the hypothesis that the signals are not overly influenced by changes in organic matter source.

### 5. Discussion

The  $\delta^{13}C_{org}$  and TOC curves across Upper Jurassic – Lower Cretaceous strata from the Buchanan Lake and Geodetic Hills sections show similar trends, and this permits confidence in

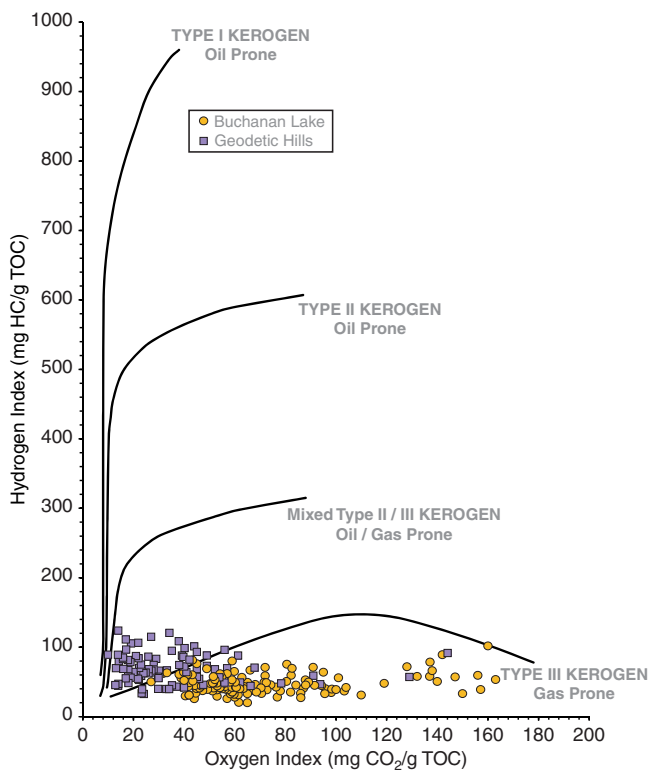


**Fig. 5.** Van Krevelen diagram of hydrogen index v. oxygen index from the Buchanan Lake and Geodetic Hills sections.

extrapolating fossil age control from the Buchanan Lake section to the Geodetic Hills section. A marked negative excursion of up to  $-4\text{‰}$ , reaching to  $-30\text{‰}$  (Fig. 4), occurs in probable middle Volgian strata of the lower Deer Bay Formation. This is followed by a return to less negative values near  $-27\text{‰}$ , a brief negative excursion of an additional  $c.1.0\text{--}1.5\text{‰}$  that may be late Volgian in age, an interval of generally increasing values and then a relatively positive carbon isotope excursion in strata of Valanginian age of the upper part of the Deer Bay Formation.

### 5.a. VOICE

Trends in  $\delta^{13}\text{C}_{\text{org}}$  from the Buchanan Lake and Geodetic Hills sections of the Deer Bay Formation are consistent with other  $\delta^{13}\text{C}_{\text{org}}$  curves spanning the Jurassic–Cretaceous boundary interval in the High Arctic (Hammer *et al.* 2012; Zakharov *et al.* 2014; Koevoets *et al.* 2016; Fig. 7). In those records, relatively positive carbon isotope values of  $c. -28\text{‰}$  are observed in the Kimmeridgian and lowest Volgian strata and are followed by an up to  $4\text{--}6\text{‰}$  more negative excursion in the middle Volgian strata. This event is followed by a return to relatively more positive values during late Volgian and Ryazanian time. Hammer *et al.* (2012) term the negative excursion they document in lower middle Volgian strata of the Slotsmøya Member (Agardhfjellet Formation) the Volgian Isotopic Carbon Excursion (VOICE). Hammer *et al.* (2012) correlate the VOICE with a lower middle Volgian broad minimum in the  $\delta^{13}\text{C}_{\text{carb}}$  record from belemnite rostra of Žák *et al.* (2011) that spans the Oxfordian–Ryazanian interval at the Nordvik Peninsula, Siberia. Hammer *et al.* (2012) also relate the VOICE to a negative excursion in  $\delta^{13}\text{C}_{\text{carb}}$  from Helmsdale, Scotland in the Sub-boreal lower middle Volgian *Rotunda–Fittoni* ammonite zone (Nunn & Price, 2010) and a negative  $\delta^{13}\text{C}_{\text{carb}}$

excursion in DSDP site 534A in the ?Tithonian strata (western central Atlantic; Katz *et al.* 2005). Hammer *et al.* (2012) conclude that the lower middle Volgian negative excursion seen in their  $\delta^{13}\text{C}_{\text{org}}$  record from Spitsbergen is consistent with carbonate records from elsewhere in the Boreal and High Boreal realms, the central Atlantic and, ‘to a lesser degree’ with the western Tethys. Koevoets *et al.* (2016) also examined the organic carbon isotope record preserved in the Upper Jurassic – Lower Cretaceous Agardhfjellet Formation of central Spitsbergen. A marked negative excursion of  $c. 4\text{‰}$  is measured and dated as middle Volgian. Koevoets *et al.* (2016) argue that the VOICE is also recognized in  $\delta^{13}\text{C}_{\text{carb}}$  curves from the Russian Platform (Price & Rogov, 2009). Zakharov *et al.* (2014) document an irregular but overall decline in  $\delta^{13}\text{C}_{\text{carb}}$  (as determined in belemnite rostra; Žák *et al.* 2011) throughout Upper Jurassic strata from the Nordvik section that they relate to a gradual increase in  $\text{CO}_2$  in the atmosphere–ocean system, and that may have led to warming based on coeval changes in a belemnite oxygen isotope record. They also present a  $\delta^{13}\text{C}_{\text{org}}$  record that shows a negative excursion of  $c. 3\text{‰}$  within the *Exoticus* Zone and extending into the basal part of the [*Craspedites*] *Okensis* Zone (late middle Volgian – early late Volgian). Trends observed in the  $\delta^{13}\text{C}_{\text{org}}$  at this locality are not observed in the  $\delta^{13}\text{C}_{\text{carb}}$  of belemnite rostra from the same section (Žák *et al.* 2011; Zakharov *et al.* 2014). Morgans-Bell *et al.* (2001) examined the Kimmeridgian–Berriasian interval of the Wessex Basin from Dorset, UK. A prominent middle Tithonian negative excursion of  $\delta^{13}\text{C}_{\text{org}}$  is not apparent in their record, although a short-lived excursion may be related to the VOICE (Turner *et al.* 2019). Turner *et al.* (2019) also interpret a short-lived decline in  $\delta^{13}\text{C}_{\text{org}}$  values in the *Pallasiodites* Zone in Core 6406/12-2 from the Norwegian Sea as the VOICE. The composite  $\delta^{13}\text{C}_{\text{carb}}$  curve from the base of the Kimmeridgian to the base of the Valanginian sections, based mostly on Tethyan data, shows no major negative carbon isotope events (Fig. 7; Price *et al.* 2016).

Decoupling of high-latitude  $\delta^{13}\text{C}_{\text{org}}$  records and Tethyan records, the latter based mostly on carbonates, suggests either that pools of organic carbon and dissolved inorganic carbon were effectively decoupled during this time, or that there was latitudinal decoupling between the Arctic and Tethyan seas. Typically, covariant marine  $\delta^{13}\text{C}_{\text{carb}}$  and  $\delta^{13}\text{C}_{\text{org}}$  are seen and interpreted as evidence that both carbonate and organic matter were originally produced in the surface waters of the ocean and retained their original  $\delta^{13}\text{C}$  composition (e.g. Kump & Arthur, 1999; Meyer *et al.* 2013). Coupled terrestrial organic (e.g. derived from fossil wood or charcoal) and carbonate records suggest strong coupling of the ocean–atmosphere system (e.g. Gröcke *et al.* 2005; Vickers *et al.* 2016), whereas decoupled  $\delta^{13}\text{C}_{\text{carb}}$  and  $\delta^{13}\text{C}_{\text{org}}$  records have been interpreted as evidence for diagenetic alteration (Meyer *et al.* 2013; Han *et al.* 2018). In these latter examples, a large negative excursion in  $\delta^{13}\text{C}_{\text{carb}}$  is typically not accompanied by a large response in the  $\delta^{13}\text{C}_{\text{org}}$  record (e.g. Fike *et al.* 2006). Alternatively, Bodin *et al.* (2016) have recently suggested lithological control on decoupling between  $\delta^{13}\text{C}_{\text{carb}}$  and  $\delta^{13}\text{C}_{\text{org}}$  records during Early Jurassic time, whereby  $\delta^{13}\text{C}_{\text{carb}}$  signatures were affected by regional variation in carbonate composition. As the Arctic middle Volgian negative event is observed in organic carbon records from Canada (this study), Spitsbergen and Siberia (Fig. 7), it is unlikely that diagenesis or regional differences in the composition of bulk organic carbon are significant factors in explaining its absence from lower-latitude areas. Instead, the absence of the negative excursion from lower-latitude carbonate records may be explained by decoupling of high-northern-latitude regions from the global carbon pool.



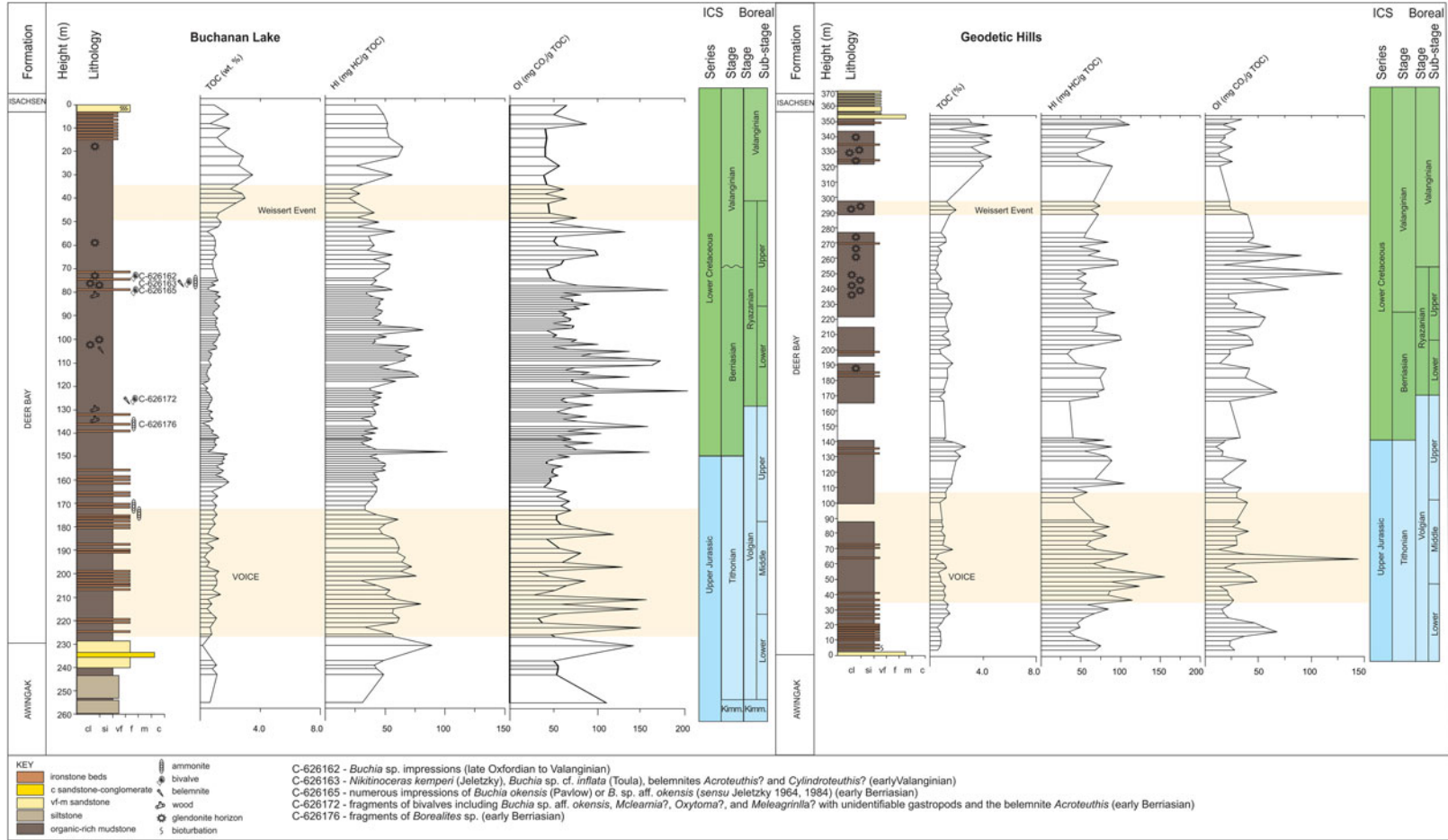


**Fig. 6.** Stratigraphic trends in Rock Eval parameters TOC, HI and OI from the Buchanan Lake and Geodetic Hills sections. Events recognized in  $\delta^{13}\text{C}_{\text{org}}$  curves are shown in yellow. The International Chronostratigraphic Chart (ICS) v 2018/08 (Cohen *et al.* 2013; updated) and Boreal Stage and Sub-stage (after Shurygin & Dzyuba *et al.* 2015) are shown.

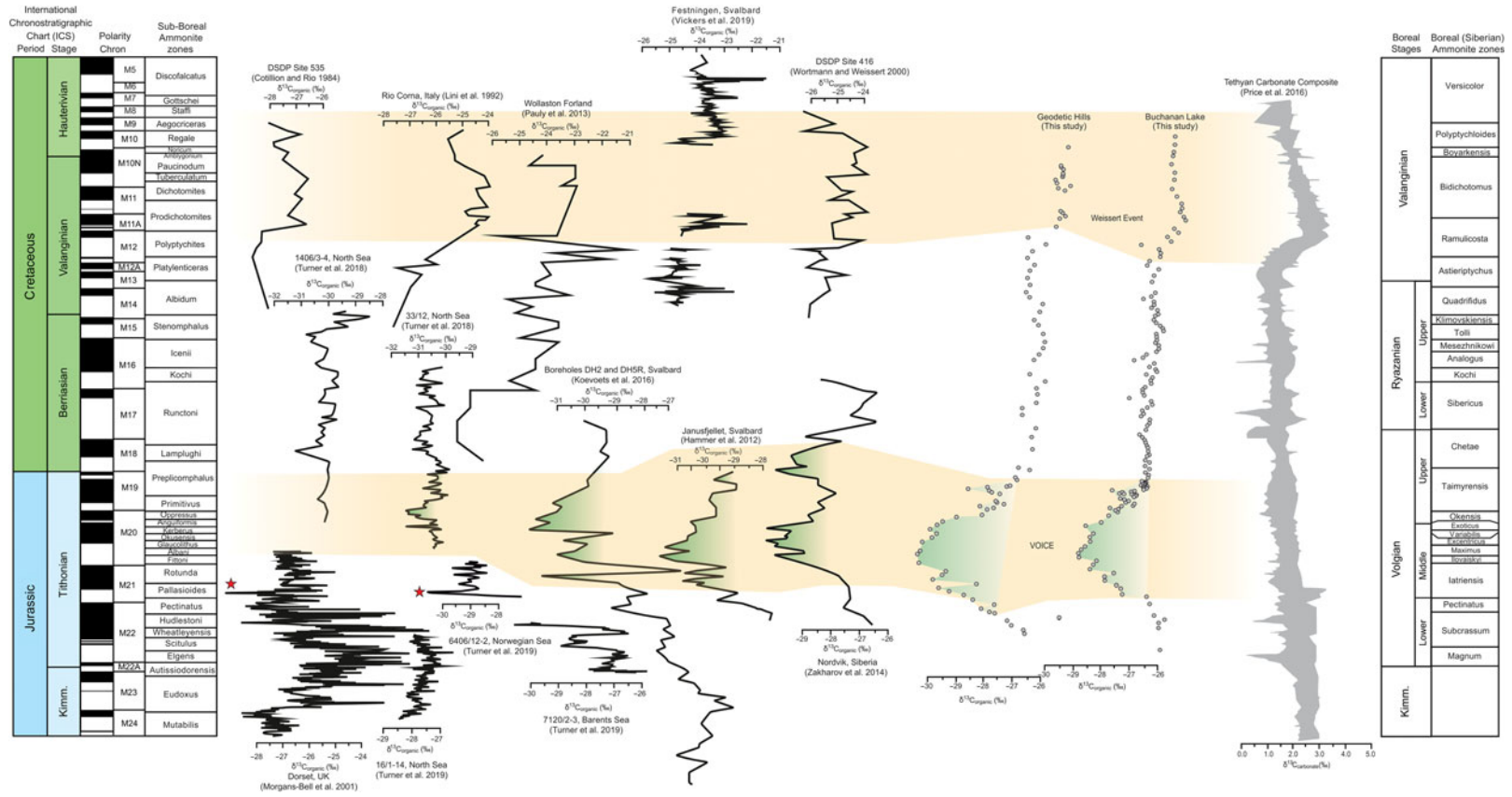


**Fig. 7.** Summary of published data for Late Jurassic – Early Cretaceous organic carbon isotope data from Atlantic and Tethyan sections, the global stack of Tethyan carbonate records and the new Arctic curves. Sub-boreal ammonite zones from Mutterlose *et al.* (2014) and Turner *et al.* (2019). Boreal (Siberian) ammonite zones after Zakharov *et al.* (1997), Baraboshkin (2004) and Shurygin & Dzyuba (2015). The International Chronostratigraphic Chart (ICS) v. 2018/08 (Cohen *et al.* 2013; updated) and Boreal Stage and Sub-stage (after Shurygin & Dzyuba *et al.* 2015) are shown. Red stars indicate levels interpreted as VOICE by Turner *et al.* (2019).

The organic carbon isotope record is influenced by a number of environmental factors (Kump & Arthur, 1999) and, as such, can be difficult to interpret (Jenkyns *et al.* 2002). Organic carbon isotope composition is strongly controlled by the type of organic matter (marine *v.* terrestrial) and, therefore, by both local and regional variables such as sea level, productivity and climate. Burial rate of organic matter enriched in  $^{12}\text{C}$  is also important, as more heavy carbon would remain in the global carbon pool. This process leads to a positive isotopic shift in both carbonates and organic matter. A decline in the  $\delta^{13}\text{C}$  value involves a relative increase in  $^{12}\text{C}$  in the oceanic carbon reservoir (Price & Gröcke, 2002). This could occur through a combination of mechanisms, including decreased carbon burial rate as a result of decreased preservation (e.g. deep basin ventilation), decreased sea-surface productivity (Weissert & Channell, 1989; Weissert & Erba, 2004), increased flux of  $^{12}\text{C}$  into surface waters by upwelling of  $^{12}\text{C}$ -rich bottom waters (Küspert, 1982) or intensified weathering and riverine input of dissolved inorganic carbon (Weissert & Mohr, 1996). A geological rapid release of  $^{12}\text{C}$  into the atmosphere associated with volcanism, methane release from dissociation of gas hydrates or combustion of organic matter associated with emplacement of large igneous bodies are other mechanisms that can cause a negative excursion in  $\delta^{13}\text{C}$  (Dickens *et al.* 1995; Hesselbo *et al.* 2000; Padden *et al.* 2001; Schröder-Adams *et al.* 2019).

A geologically sudden increase in volcanism could potentially explain the large negative  $\delta^{13}\text{C}_{\text{org}}$  values seen in the middle Volgian Arctic records and an absence from  $\delta^{13}\text{C}_{\text{carb}}$  records (Price *et al.* 2016). As modelled by Kump & Arthur (1999), an increase in volcanism sufficient to perturb atmospheric  $p\text{CO}_2$  levels could drive down the carbon isotopic value in the ocean–atmosphere system. However, any trend in  $\delta^{13}\text{C}_{\text{carb}}$  could be relatively quickly countered as burial of anomalously depleted organic matter may overcompensate for additional input of depleted volcanic  $\text{CO}_2$  (Kump & Arthur, 1999). Notwithstanding this, the Shatsky Rise, a vast shield volcano with a surface area of *c.* 480 000 km<sup>2</sup>, formed in the NW Pacific Ocean at about the Jurassic–Cretaceous boundary (Sager *et al.* 2013). Recent  $^{40}\text{Ar}/^{39}\text{Ar}$  age determinations of basaltic lava samples from Tamu Massif, the oldest and largest edifice of the submarine Shatsky Rise, provide an age of *c.* 144 Ma (Geldmacher *et al.* 2014), similar to the widely used *c.* 145 Ma  $^{40}\text{Ar}/^{39}\text{Ar}$  minimum age for the Jurassic–Cretaceous boundary proposed by Mahoney *et al.* (2005). However, new U–Pb ages from Argentina and Mexico suggest that the numerical age of the Jurassic–Cretaceous boundary may lie between 140.7 and 140.9 Ma; this evidence would place an age of *c.* 145 Ma (the current ICS age for the base of the Berriasian stage) into the middle of the Tithonian age (Lena *et al.* 2019), whether the base of the Tithonian is 152.1 Ma (Cohen *et al.* 2013; updated 2018/08) or 148 Ma (Lena *et al.* 2019) or somewhere between. Sub-aerial volcanism and summit weathering and/or erosion of the emergent phase of the Shatsky Rise is thought to have occurred as early as during the Valanginian age (Yasuhara *et al.* 2017), suggesting possible further complications in the interpretation of significance of the age of the sills associated with the Shatsky Rise. The ages of the base of the Tithonian and Berriasian stages are yet to be confirmed (e.g. Ogg & Hinnov, 2012; Aguirre-Urreta *et al.* 2015).

Hydrocarbon seeps are widely distributed in Upper Jurassic and Jurassic–Cretaceous boundary beds in Spitsbergen. Seeps characterized by authigenic carbonates in the uppermost Jurassic Slottsmøya Member of the Agardhfjellet Formation in the Sassenfjorden area of central Spitsbergen (Hammer *et al.* 2011) may be related to the release of gas hydrates (Kiel, 2009),

early thermal steepening of the geothermal gradient and/or tectonic activity associated with the initial phases of High Arctic Large Igneous Province (HALIP) activity (Maher, 2001; Hammer *et al.* 2011). HALIP, a major magmatic event, may therefore be relevant to the VOICE carbon isotope record, although the currently known ages of the HALIP intrusives are younger than those of the VOICE, ranging from 95–91 Ma to *c.* 127 Ma (Omma *et al.* 2011; Evenchick *et al.* 2015; Dockman *et al.* 2018; Kingsbury *et al.* 2018; Fig. 2). Seep carbonates are also found in the Janusfjellet section of Spitsbergen; these are of late Volgian – earliest Valanginian age (Wierzbowski *et al.* 2011), and are therefore younger than the carbon isotope excursion documented in Sverdrup Basin.

Eustatic sea-level fall was invoked by Nunn & Price (2010) to explain a general trend towards more negative  $\delta^{13}\text{C}_{\text{carb}}$  values in their belemnite record from Helmsdale, Scotland, in the Tithonian Stage. A sea-level fall could result in enhanced release of  $^{12}\text{C}$  from weathering, erosion and oxidation of organic-rich sub-aerially exposed rock (Voigt & Hilbrecht, 1997; Price & Gröcke, 2002) as well as compositional deviation away from open-marine  $\delta^{13}\text{C}$  values in relatively isolated epicontinental seas (e.g. Holmden *et al.* 1998; Immenhauser *et al.* 2003). ‘Local’ depletion in  $^{13}\text{C}$  is caused by isotopically light  $\text{CO}_2$  input from respiration of marine organisms, as well as oxidation of terrestrial organic matter and input of isotopically light riverine dissolved inorganic carbon (Patterson & Walter, 1994; Holmden *et al.* 1998). Progressive oxidation of organic matter to  $\text{CO}_2$  (‘sea water aging’, Holmden *et al.* 1998), which then forms dominantly bicarbonate in sea water, is greatest during a long residence time of water masses in shallow, poorly circulated settings (Patterson & Walter, 1994). The uptake of this bicarbonate in carbonates or marine organic matter in isotopic equilibrium with dissolved inorganic carbon results in carbonate or organic materials with depleted  $\delta^{13}\text{C}$  values.

The Deer Bay Formation is the result of regional marine transgression that was preceded by a sea-level lowstand in Sverdrup Basin (Embry & Beauchamp, 2019), with restricted marine connections and a large number of restricted environments (e.g. Ziegler, 1988; Hardenbol *et al.* 1998). The Deer Bay rift climax of the Sverdrup Basin occurred during this time and basin subsidence was associated with contemporaneous rift margin uplift (Hadlari *et al.* 2016). Due to low global sea-level during the Tithonian Age, the only direct connection between the North Atlantic and the Sverdrup Basin was the narrow and shallow Norwegian–Greenland Seaway, which was more than 1500 km long and only 200–300 km wide (Ziegler, 1988; Dore, 1991). Connections between the western Sverdrup Basin and Panthalassa were similarly constricted prior to rift-opening of the Canada Basin in the Hauterivian Age (e.g. Embry & Beauchamp, 2019). The Sverdrup Basin and other high-latitude Boreal basins (e.g. Dypvik & Zakharov, 2012) could have experienced compositional evolution away from global marine  $\delta^{13}\text{C}$  values during middle Volgian time, but effectively became re-coupled by Valanginian time due to global sea-level rise. The hypothesis of restriction of Sverdrup Basin water masses during Volgian time, followed by more open circulation during Valanginian time, is consistent with global sea-level fluctuations (Haq *et al.* 2017), and may be supported by the greater number of known ammonite occurrences in the Valanginian part of the Deer Bay Formation, and the greater similarity of faunas between the Arctic and Europe at this time relative to the Late Jurassic. Embry (1991, p. 408, 414) noted three transgressive–regressive cycles during the Kimmeridgian – late Berriasian interval in the Sverdrup Basin, a gradual decline in sediment supply and a shift of the basin axis to the west, with

sandstones occupying the basin margins. Sea-level rise during Early Cretaceous time would have increased ventilation of the incipient Arctic Ocean and thus coupled the carbon dynamics of the Sverdrup Basin to the open-marine system. This interpretation would imply a similar oceanographic restriction to explain the middle Volgian negative  $\delta^{13}\text{C}$  events in Svalbard and Siberia. It might also partly explain and support the ongoing difficulties with correlating Tethyan and Boreal marine faunas, especially if exacerbated by concurrent climate-influenced biogeographic differentiation.

### 5.b. Weissert Event

A particularly prominent feature of Early Cretaceous global carbon isotope records is the Valanginian (Weissert)  $\delta^{13}\text{C}$  positive excursion (Lini *et al.* 1992; Price *et al.* 2016). This isotope event is widely documented in marine carbonates, fossil shell material, terrestrial plants and marine organic matter (e.g. Lini *et al.* 1992; Gröcke *et al.* 2005; Aguirre-Urreta *et al.* 2008; Price *et al.* 2016). Marine organic matter (Lini *et al.* 1992; Wortmann & Weissert, 2000) typically shows a c. 2‰ excursion. Despite the noisy pattern seen in these published records, which possibly relate to changes in the composition of the bulk organic carbon, the shape of the  $\delta^{13}\text{C}$  curve is characterized by a rapid rise from the pre-excursion background, a plateau and a less steep decline to a new steady state that is slightly more positive than prior to the event. Only in the record from Greenland is the Valanginian (Weissert)  $\delta^{13}\text{C}$  positive excursion less clear, possibly due to condensation of the strata and related sample density, or a hiatus in the sedimentary record (Pauly *et al.* 2013). Given the overall pattern and magnitude of the excursions in the marine records, the positive carbon isotope excursion of up to 1.5‰ in the upper part of the Deer Bay Formation is interpreted to represent the Valanginian (Weissert) event in Arctic Canada.

## 6. Conclusions

Carbon isotope stratigraphy from two sections in the Canadian High Arctic that span the Jurassic–Cretaceous boundary documents a marked middle Volgian negative excursion with a magnitude of c. 4‰ followed by a return to less negative values. A positive excursion is evident with a magnitude of c. 1.5‰ in the Valanginian Stage. The Volgian isotopic trends are consistent with other high-latitude records but are decoupled from Tethyan  $\delta^{13}\text{C}_{\text{carb}}$  records. The globally recognized isotopically positive Weissert Event in the Valanginian Stage is also recognized in the Canadian Arctic sections. The Sverdrup Basin and other Arctic basins may have experienced compositional evolution away from open-marine  $\delta^{13}\text{C}$  values during the middle Volgian Age in relatively isolated basins due to low global sea levels, and became effectively re-coupled by Valanginian time when global sea level rose. As well as providing another correlation tool in a time interval with challenging inter-provincial biostratigraphic correlations, C isotope excursions such as those presented here offer further insight into the causes of major global ocean–atmosphere perturbations beyond the conventional volcanic interpretation.

**Acknowledgements.** Financial support for field work and analyses was provided by the GeoMapping for Energy and Minerals (GEM) Program (Natural Resources Canada, Geological Survey of Canada). Collections and research on those collections were made under the Government of Nunavut Archaeology and Palaeontology Research Permit 2015-03P. Data analyses and production of this research paper were conducted at the Geological Survey of Canada and at the Aarhus Institute of Advanced Studies at Aarhus

University. JMG received funding from the AIAS-COFUND II fellowship programme that is supported by the Marie Skłodowska-Curie actions under the European Union's Horizon 2020 (grant agreement no. 754513) and the Aarhus University Research Foundation. We are grateful to Dr Keith Dewing for project management and Dr Lisa Neville (Calgary, AB) and Pilipoosie Iqaluk (Hamlet of Resolute Bay, NU) for assistance with sample collection and field logistics. We acknowledge the logistics support provided by the Polar Continental Shelf Program (NRCan) and UHL Helicopters (Pilot Lorne Pike). We are grateful for the staff of the Environment and Climate Change Canada Eureka Weather Station and, in particular, Station Manager André Beauchard. Dr Mikhail Rogov particularly, as well as Drs Aleksandr Igolnikov and Victor Zakharov, offered important advice concerning the current taxonomic assignments and ages of the ammonites and a *Buchia* specimen. Glen Edwards produced the photographs and the fossil plate. This publication represents NRCan Contribution Number/Numéro de contribution de RNCAN 20190001. We are grateful for the comments of Dr Manuel Bringué (Geological Survey of Canada) for his internal review and to Dr Øyvind Hammer and Dr Mikhail Rogov for detailed external reviews that greatly improved this contribution. We also thank the Editor Dr Bas Van de Schootbrugge for comments and suggestions.

**Supplementary material.** To view supplementary material for this article, please visit <https://doi.org/10.1017/S0016756819001316>.

## References

- Aguirre-Urreta MB, Lescano M, Schmitz MD, Tunik M, Concheyro A, Rawson PF and Ramos VA (2015) Filling the gap: new precise Early Cretaceous radioisotopic ages from the Andes. *Geological Magazine* **152**, 557–64.
- Aguirre-Urreta MB, Naipauer M, Lescano M, López-Martínez R, Pujana I, Vennari V, De Lena LF, Concheyro A and Ramos VA (2019) The Tithonian chrono-biostratigraphy of the Neuquén Basin, Argentine Andes: a review and update. *Journal of South American Earth Sciences* **92**, 350–67.
- Aguirre-Urreta MB, Price GD, Ruffell AH, Lazo DG, Kalin RM, Ogle N and Rawson PF (2008) Southern hemisphere Early Cretaceous (Valanginian–Early Barremian) carbon and oxygen isotope curves from the Neuquén basin, Argentina. *Cretaceous Research* **29**, 87–99.
- Alroy J (2010) Geographical, environmental and intrinsic biotic controls on Phanerozoic marine diversification. *Palaeontology* **53**, 1211–35.
- Amato JM, Toro J, Akinin VV, Hampton BA, Salnikov AS and Tuckkova MI (2015) Tectonic evolution of the Mesozoic South Anyui suture zone, eastern Russia: a critical component of paleogeographic reconstructions of the Arctic region. *Geosphere* **11**, 1530–64.
- Aradkani OH, Sanei H, Snowdon LR, Outridge PM, Obermajer M, Stewart R, Vandenberg R and Boyce K (2016) The accepted values for the internal Geological Survey of Canada (GSC) 9107 Rock-Eval 6<sup>®</sup> standard (Upper Cretaceous Second White Speckled Shale, Colorado Group), western Canada. *Geological Survey of Canada*, Open File no. 8043, 9 p. doi: [10.4095/298729](https://doi.org/10.4095/298729)
- Balkwill HR (1978) Evolution of Sverdrup Basin, Arctic Canada. *Bulletin of AAPG* **62**, 1004–28.
- Balkwill HR (1983) *Geology of Amund Ringnes, Cornwall, and Haig-Thomas Islands, District of Franklin*. Geological Survey of Canada, Ottawa, Memoir no. 390, 76 p.
- Balkwill HR, Wilson DG and Wall JH (1977) Ringnes Formation (Upper Jurassic), Sverdrup Basin, Canadian Arctic Archipelago. *Bulletin of Canadian Petroleum Geology* **25**, 1115–43.
- Baraboshkin EY (2004) Boreal-Tethyan correlation of Lower Cretaceous ammonite scales. *Moscow University Geology Bulletin* **59**(6), 9–20.
- Bodin S, Krencker F, Kothe T, Hoffmann R, Mattioli E, Heimhofer U and Kabiri L (2016) Perturbation of the carbon cycle during the late Pliensbachian – Early Toarcian: new insight from high-resolution carbon isotope records in Morocco. *Journal of African Earth Sciences* **116**, 89–104.
- Bragin VY, Dzyuba OS, Kazansky AY and Shurygin BN (2013) New data on the magnetostratigraphy of the Jurassic-Cretaceous boundary interval, Nordvik Peninsula (northeastern East Siberia). *Russian Geology and Geophysics* **54**, 335–48.

- Cohen KM, Finney SC, Gibbard PL and Fan J-X (2013) The ICS International Chronostratigraphic Chart. *Episodes* **36**, 199–204; online update <http://www.stratigraphy.org/ICSchart/ChronostratChart2018-08.jpg>
- Cotillion P and Rio M (1984) Calcium carbonate, isotopes and Rock-Eval pyrolysis at DSDP Holes 77-535 and 77-540. Supplement to Cyclic sedimentation in the Cretaceous of Deep Sea Drilling Project Sites 535 and 540 (Gulf of Mexico), 534 (Central Atlantic), and in the Vocontian Basin (France). In *Initial Reports of the Deep Sea Drilling Project vol. 77* (eds Buffler RT and Schlager W), pp. 339–76. Washington: US Government Printing Office.
- Davis WJ, Schröder-Adams C, Galloway JM, Herrle J and Pugh A (2016) U-Pb geochronology of bentonites from the Upper Cretaceous Kanguk Formation, Sverdrup Basin, Arctic Canada: Constraints on sedimentation rates, biostratigraphic correlations and the late magmatic history of the High Arctic Large Igneous Province. *Geological Magazine* **154**, 757–76.
- Dewing K, Turner E and Harrison JC (2007) Geological history, mineral occurrences and mineral potential of the sedimentary rocks of the Canadian Arctic Archipelago. In *Mineral Deposits of Canada: A Synthesis of Major Deposit-Types, District Metallogeny, the Evolution of Geologic Provinces, and Exploration Methods* (ed. WD Goodfellow), p. 733–53. Geological Association of Canada, St John's, Mineral Deposits Division, Special Publication no. 5.
- Dickens GR, O'Neil JR, Rea DK and Owen RM (1995) Dissociation of oceanic methane hydrate as a cause of the carbon isotope excursion at the end of the Paleocene. *Paleoceanography and Paleoclimatology* **10**, 965–71.
- Dockman DM, Pearson DG, Heaman LM, Gibson SA, Sarkar C (2018) Timing and origin of magmatism in the Sverdrup Basin, Northern Canada – Implications for lithospheric evolution in the High Arctic Large Igneous Province (HALIP). *Tectonophysics* **742–743**, 50–65.
- Dore AG (1991) The structural foundation and evolution of Mesozoic seaways between Europe and the Arctic Sea. *Palaeogeography, Palaeoclimatology, Palaeoecology* **87**, 441–92.
- Dypvik H and Zakharov V (2012) Fine grained epicontinental Arctic sedimentation – mineralogy and geochemistry of shales from the Late Jurassic–Early Cretaceous transition. *Norwegian Journal of Geology* **92**, 65–87.
- Dzyuba OS, Izokh OP and Shurygin BN (2013) Carbon isotope excursions in Boreal Jurassic–Cretaceous boundary sections and their correlation potential. *Palaeogeography, Palaeoclimatology, Palaeoecology* **381–382**, 33–46.
- Embry AF (1985) New stratigraphic units, Middle Jurassic to lowermost Cretaceous succession, Arctic Islands. Geological Survey of Canada, Ottawa, Current Research Paper no. 85-1b, p. 269–76.
- Embry AF (1991) Mesozoic history of the Arctic Islands. In *Innuitian Orogen and Arctic Platform of Canada and Greenland* (ed. H Trettin), pp. 369–433. Geological Survey of Canada, Ottawa.
- Embry AF (2011) Petroleum prospectivity of the Triassic–Jurassic succession of Sverdrup Basin, Canadian Arctic Archipelago. In *Arctic Petroleum Geology* (eds AM Spencer, AF Embry, DL Gautier, AV Stoupakova and K Sørensen), pp. 545–58. Geological Society of London, Memoir no. 35.
- Embry AF and Beauchamp B (2019) Chapter 14 Sverdrup Basin. In *The Sedimentary Basins of the United States and Canada*, 2nd Edition (ed. A Miall), p. 559–92. Amsterdam: Elsevier.
- Erba E, Bartolini A and Larson RL (2004) Valanginian Weissert oceanic anoxic event. *Geology* **32**, 149–52.
- Evenchick CA, Davis WJ, Bédard JH, Hayward N and Friedman RM (2015) Evidence for protracted High Arctic large igneous province magmatism in the central Sverdrup Basin from stratigraphy, geochronology, and paleodepths of saucer-shaped sills. *Geological Society of America Bulletin* **127**, 1366–90.
- Fike DA, Grotzinger JP, Pratt LM and Summons RE (2006) Oxidation of the Ediacaran Ocean. *Nature* **444**, 744–7.
- Galloway JM, Sweet A, Sanei H, Dewing K, Hadlari T, Embry AF and Swindles GT (2013) Middle Jurassic to Lower Cretaceous paleoclimate of Sverdrup Basin, Canadian Arctic Archipelago inferred from the palynostratigraphy. *Marine and Petroleum Geology* **44**, 240–55.
- Geldmacher J, van den Bogaard P, Heydolph K and Hoernle K (2014) The age of Earth's largest volcano: Tamu Massif on Shatsky Rise (northwest Pacific Ocean). *International Journal of Earth Sciences* **103**, 2351–7.
- Grasby SE, McCune GE, Beauchamp B and Galloway JM (2017) Lower Cretaceous cold snaps led to widespread glendonite occurrences in the Sverdrup Basin, Canadian High Arctic. *Geological Society of America Bulletin* **129**, 771–878.
- Gröcke DR, Price GD, Robinson SA, Baraboshkin EY, Mutterlose J and Ruffell AH (2005) The Upper Valanginian (Early Cretaceous) positive carbon-isotope event recorded in terrestrial plants. *Earth and Planetary Science Letters* **240**, 495–509.
- Hadlari T, Dewing K, Matthews WA, Alonson-Torres D and Midwinter D (2018) Early Triassic development of a foreland basin the Canadian high Arctic: Implications for a Pangean Rim of Fire. *Tectonophysics* **736**, 75–84.
- Hadlari T, Midwinter D, Galloway JM, Durban AM (2016) Mesozoic rift to post-rift tectonostratigraphy of the Sverdrup Basin, Canadian Arctic. *Marine and Petroleum Geology* **76**, 148–58.
- Hadlari T, Midwinter D, Poulton TP and Matthews WA (2017) A Pangean rim of fire: Reviewing the Triassic of western Laurentia. *Lithosphere* **9**, 579–82.
- Hallam A (1986) The Pliensbachian and Tithonian extinction events. *Nature* **319**, 765–8.
- Hammer Ø, Collignon M and Nakrem HA (2012) Organic carbon isotope chemostratigraphy and cyclostratigraphy in the Volgian of Svalbard. *Norwegian Journal of Geology* **92**, 103–12.
- Hammer Ø, Nakrem HA, Little CTS, Hryniewicz K, Sandy MR, Hurum JH, Druckenmiller P, Knutsen EM and Høyberget M (2011) Hydrocarbon seeps from close to the Jurassic–Cretaceous boundary, Svalbard. *Palaeogeography, Palaeoclimatology, Palaeoecology* **306**, 15–26.
- Han Z, Hu X, Kemp DB and Li J (2018) Carbonate platform response to the Toarcian Oceanic Anoxic Event in the southern hemisphere: Implications for climatic change and biotic platform demise. *Earth and Planetary Science Letters* **489**, 59–71.
- Haq BU (2017) Jurassic sea-level variations: a reappraisal. *GSA Today* **28**, no. 1, doi: [10.1130/GSATG359A.1](https://doi.org/10.1130/GSATG359A.1).
- Hardenbol J, Thierry J, Farley MB, Jacquin T, de Graciansky P-C and Vail PR (1998) Mesozoic and Cenozoic sequence chronostratigraphic framework of European basins. In *Mesozoic and Cenozoic Sequence Stratigraphy of European Basins* (eds P-C de Graciansky, J Hardenbol, T Jacquin and PR Vail), p. 3–13, charts 1–8. Society for Sedimentary Geology (SEPM), Tulsa, Special Publication no. 60.
- Herrle J, Schröder-Adams CJ, Davis W, Pugh AT, Galloway JM and Fath J (2015) Mid-Cretaceous High Arctic stratigraphy, climate and Oceanic Anoxic Events. *Geology* **43**, 403–6.
- Hesselbo SP, Gröcke DR, Jenkyns HC, Bjerrum CJ, Farrimond P, Morgans Bell HS and Green OR (2000) Massive dissociation of gas hydrate during a Jurassic oceanic anoxic event. *Nature* **406**, 392–5.
- Heywood WW (1957) Isachsen area, Ellef Ringnes Island, District of Franklin, Northwest Territories. Geological Survey of Canada, Ottawa, Paper no. 56–8, 36 p.
- Holmden CE, Creaser RA, Muehlenbachs K, Leslie SA and Bergström SM (1998) Isotopic evidence for geochemical decoupling between ancient epicirc seas and bordering oceans: Implications for secular curves. *Geology* **26**, 567–70.
- Houša V, Pruner P, Zakharov VA, Košťák M, Chadima M, Rogov MA, Šlechtá S and Mazuch M (2007) Boreal-Tethyan correlation of the Jurassic–Cretaceous boundary interval by magnetostratigraphy and biostratigraphy. *Stratigraphy Geological Correlation* **15**, 297–309.
- Hunt JM (1996) *Petroleum Geochemistry and Geology*, 2nd Edition. New York: WH Freeman and Co., 743 pp.
- Immenhauser A, della Porta G, Kenter JAM and Bahamonde JR (2003) An alternative model for positive shifts in shallow-marine carbonate  $\delta^{13}\text{C}$  and  $\delta^{18}\text{O}$ . *Sedimentology* **50**, 953–59.
- Jeletzky JA (1964) Illustrations of Canadian Fossils. Lower Cretaceous marine index fossils of the sedimentary basins of western and Arctic Canada. Geological Survey of Canada, Ottawa, Paper no. 64-11 (101 p., 36 plates).
- Jeletzky JA (1973) Biochronology of the marine boreal latest Jurassic, Berriasian and Valanginian in Canada. *Geological Journal Special Issue* no. 5, 41–80.
- Jeletzky JA (1984) Jurassic–Cretaceous boundary beds of western and Arctic Canada and the problem of the Tithonian–Berriasian stages in the Boreal Realm. In *Jurassic–Cretaceous Biochronology and Paleogeography of North*

- America (ed. GEG Westernamm), p. 175–254. Geological Association of Canada, St John's, Special Paper no. 27.
- Jenkyns HC, Jones CE, Gröcke DR, Hesselbo SP and Parkinson DN** (2002) Chemostratigraphy of the Jurassic system: applications, limitations and implications for palaeoceanography. *Journal of the Geological Society of London* **159**, 351–78.
- Katz ME, Wright JD, Miller KG, Cramer BS, Fennel K and Falkowski PG** (2005) Biological overprint of the geological carbon cycle. *Marine Geology* **217**, 323–38.
- Kemper E** (1975) Upper Deer Bay Formation (Berriasian-Valanginian) of Sverdrup Basin and biostratigraphy of the Arctic Valanginian. Geological Survey of Canada, Ottawa, Paper no. 75-1B, p. 245–54.
- Kemper E** (1977) Biostratigraphy of the Valanginian in Sverdrup Basin, District of Franklin. Geological Survey of Canada, Ottawa, Paper no. 76–32, 6 p.
- Kemper E** (1983) Über Kalt- und Warmzeiten der Unterkreide. *Zitteliana* **10**, 359–69.
- Kemper E** (1987) Das Klima der Kreide-Zeit. *Geologisches Jahrbuch* **A96**, 5–185.
- Kemper E and Jeletzky JA** (1979) New stratigraphically and phylogenetically important oolostephanid (Ammonitida) taxa from the uppermost Lower and Upper Valanginian of Sverdrup Basin, Northwest Territories. Geological Survey of Canada, Ottawa, Paper no. 79–19, 25p.
- Kemper E and Schmitz HH** (1975) Stellate nodules from the upper Deer Bay Formation (Valanginian) of Arctic Canada. Geological Survey of Canada, Ottawa, Paper no. 75-1C, p. 109–119.
- Kiel S** (2009) Global hydrocarbon seep carbonate precipitation correlates with deep-water temperatures and eustatic sea-level fluctuations since the Late Jurassic. *Terra Nova* **21**, 279–84.
- Kingsbury C, Kamo SL, Ernst RE, Söderlund U and Cousens BL** (2018) U-Pb geochronology of the plumbing system associated with the Late Cretaceous Strand Fiord Formation, Axel Heiberg Island, Canada: part of the 130–90 Ma High Arctic Large Igneous Province. *Journal of Geodynamics* **118**, 106–17.
- Koevoets MJ, Abay TB, Hammer Ø and Olausen S** (2016) High-resolution organic carbon-isotope stratigraphy of the Middle Jurassic–Lower Cretaceous Agardhfjellet Formation of central Spitsbergen, Svalbard. *Palaeogeography, Palaeoclimatology, Palaeoecology* **449**, 266–74.
- Kump LR and Arthur MA** (1999) Interpreting carbon-isotope excursions: carbonates and organic matter. *Chemical Geology* **161**, 181–98.
- Küspert W** (1982) Environmental changes during oil shale deposition as deduced from stable isotope ratios. In *Cyclic and Event Stratification* (eds G Einsele and A Seilacher), pp. 482–501. Springer, Heidelberg.
- Lena I, López-Martínez R, Lescano M, Aguirre-Urreta B, Concheyro A, Vennari V, Naipauer M, Samankassou E, Pimentel M, Ramos VA and Schaltegger U** (2019) High-precision U-Pb ages in the early Tithonian to early Berriasian and implications for the numerical age of the Jurassic-Cretaceous boundary. *Solid Earth* **10**, 1–14.
- Lini A, Weissert H and Erba E** (1992) The Valanginian carbon isotope event: a first episode of greenhouse climate conditions during the Cretaceous. *Terra Nova* **4**, 374–84.
- Maher DM Jr** (2001) Manifestations of the High Arctic Large Igneous Province in Svalbard. *Journal of Geology* **109**, 91–104.
- Mahoney JJ, Duncan RA, Tejada MLG, Sager WW and Bralower TJ** (2005) Jurassic-Cretaceous boundary age and mid-ocean-ridge-type mantle source for Shatsky Rise. *Geology* **33**, 185–8.
- Meyer KM, Yu M, Lehrmann D, van de Schootbrugge B and Payne JL** (2013) Constraints on early Triassic carbon cycle dynamics from paired organic and inorganic carbon isotope records. *Earth and Planetary Science Letters* **361**, 429–35.
- Michalík J, Reháková D, Halášová E and Lintnerová O** (2009) The Brodno section – a potential regional stratotype of the Jurassic/Cretaceous boundary (Western Carpathians). *Geological Carpathica* **60**, 213–32.
- Midwinter D, Hadlari T, Davis WJ, Dewing K and Arnott RWC** (2016) Dual provenance signatures of the Triassic northern Laurentian margin from detrital zircon U-Pb and Hf isotope analysis of Triassic-Jurassic strata in the Sverdrup Basin. *Lithosphere* **8**, 668–83.
- Morgans-Bell HS, Coe AL, Hesselbo SP, Jenkyns HC, Weedon GP, Marshall JEA, Tyson RV and Williams CJ** (2001) Integrated stratigraphy of the Kimmeridge Clay Formation (Upper Jurassic) based on exposures and boreholes in south Dorset, UK. *Geological Magazine* **138**, 511–39.
- Mountjoy EW and Procter RM** (1969) Eleven descriptions of Jurassic-Cretaceous rocks in Arctic plateau and Arctic coastal plain. Geological Survey of Canada, Ottawa, Open File 16, 65p.
- Mutterlose J, Bodin S and Fähnrich L** (2014) Strontium-isotope stratigraphy of the Early Cretaceous (Valanginian–Barremian). Implications for Boreal–Tethys correlation and paleoclimate. *Cretaceous Research* **50**, 252–63.
- Nunn EV and Price GD** (2010) Late Jurassic (Kimmeridgian–Tithonian) stable isotopes ( $\delta^{18}\text{O}$ ,  $\delta^{13}\text{C}$ ) and Mg/Ca ratios: new palaeoclimate data from Helmsdale, northeast Scotland. *Palaeogeography, Palaeoclimatology, Palaeoecology* **292**, 325–35.
- Ogg JG and Hinnov LA** (2012) Jurassic. Chapter 26. In *The Geologic Time Scale 2012* (eds FM Gradstein, JG Ogg, MD Schmitz and GM Ogg), p. 731–91. Elsevier, Boston.
- Ogg JG and Lowrie W** (1986) Magnetostratigraphy of the Jurassic/Cretaceous boundary. *Geology* **14**, 547–50.
- Omnia JE, Pease V and Scott RA** (2011) U–Pb SIMS zircon geochronology of Triassic and Jurassic sandstones on northwestern Axel Heiberg Island, northern Sverdrup Basin, Arctic Canada. In *Arctic Petroleum Geology* (eds AM Spencer, AF Embry, DL Gautier, AV Stoupakova and K Sørensen), p. 559–66. Geological Society of London, Memoir no. 35.
- Padden M, Weissert H and de Rafelis M** (2001) Evidence for Late Jurassic release of methane from gas hydrate. *Geology* **29**, 223–6.
- Patterson WP and Walter LM** (1994) Depletion of  $^{13}\text{C}$  in seawater  $\Sigma\text{CO}_2$  on modern carbonate platforms: Significance for the carbon isotopic record of carbonates. *Geology* **22**, 885–8.
- Pauly S, Mutterlose J and Alsen P** (2013) Depositional environments of Lower Cretaceous (Ryazanian–Barremian) sediments from Wollaston Forland and Kuhn Ø, North-East Greenland. *Geological Society of Denmark, Bulletin* **61**, 19–36.
- Poulton TP** (1994) Jurassic stratigraphy and fossil occurrences – Melville, Prince Patrick, and Borden Islands. In *The Geology of Melville Island* (eds RL Christie and NJ McMillan), p. 161–193. Geological Survey of Canada, Ottawa, Bulletin no. 450.
- Poulton TP** (1996) Chapter 10 Jurassic. In *The Geology, Mineral and Hydrocarbon Potential of Northern Yukon Territory and Northwestern District of Mackenzie* (ed DK Norris), p. 267–299. Geological Survey of Canada, Ottawa, Bulletin no. 422.
- Price GD and Gröcke DR** (2002) Strontium-isotope stratigraphy and oxygen- and carbon-isotope variation during the Middle Jurassic–Early Cretaceous of the Falkland Plateau, South Atlantic. *Palaeogeography, Palaeoclimatology, Palaeoecology* **183**, 209–22.
- Price GD, Fózy I and Pálffy J** (2016) Carbon cycle history through the Jurassic–Cretaceous boundary: A new global  $\delta^{13}\text{C}$  stack. *Palaeogeography, Palaeoclimatology, Palaeoecology* **451**, 46–61.
- Price GD and Rogov MA** (2009) An isotopic appraisal of the Late Jurassic greenhouse phase in the Russian Platform. *Palaeogeography, Palaeoclimatology, Palaeoecology* **273**, 41–9.
- Rogov MA, Ershova VB, Shchepetova EV, Zakharov VA, Pokrovsky BG and Khudoley AK** (2017) Earliest Cretaceous (late Berriasian) glendonites from Northeast Siberia revise the timing of initiation of transient Early Cretaceous cooling in the high latitudes. *Cretaceous Research* **71**, 302–112.
- Sager WW, Zhang J, Korenaga J, Sano T, Koppers AAP, Widdowson M, and Mahoney JJ** (2013) An immense shield volcano within the Shatsky Rise oceanic plateau, northwest Pacific Ocean. *Nature Geoscience* **6**, 976–81.
- Schnabl P, Pruner P and Wimbledon WAP** (2015) A review of magnetostratigraphic results from the Tithonian–Berriasian of Nordvik (Siberia) and possible biostratigraphic constraints. *Geologica Carpathia* **66**, 487–98.
- Schneider S, Kelly SA, Mutterlose J, Hulse P and Lopez-Mir B** (2019) Frosty times in the Sverdrup Basin: The Jurassic–Cretaceous transition in the Rollrock Section, Canadian Arctic Archipelago. In *JK2018 – Proceedings of International Meeting around the Jurassic-Cretaceous Boundary* (ed B Granier), p. 75–76. Carnets de Géologie, Madrid, Book 2019/01 (CG2019\_B01).

- Schröder-Adams CJ, Herrle JO, Selby D, Quesnel A and Froude G** (2019) Influence of the High Arctic Igneous Province on the Cenomanian/Turonian boundary interval, Sverdrup Basin, High Canadian Arctic. *Earth and Planetary Science Letters* **511**, 76–88.
- Scotese CR** (2014) *Atlas of Plate Tectonic Reconstructions (Mollweide Projection)*, Volumes 1–6, PALEOMAP Project PaleoAtlas for ArcGIS, PALEOMAP Project, Evanston, IL.
- Selmeier A and Grosser D** (2011) Lower Cretaceous conifer drift wood from Sverdrup Basin, Canadian Arctic Archipelago. *Zitteliana* **51**, 19–35.
- Shurygin BN and Dzyuba OS** (2015) The Jurassic/Cretaceous boundary in northern Siberia and Boreal-Tethyan correlation of the boundary beds. *Russian Geology and Geophysics* **56**, 652–62.
- Souther JG** (1963) Geological traverse across Axel Heiberg Island from Buchanan Lake to Strand Fiord. In *Geology of the North-Central Part of the Arctic Archipelago, Northwest Territories (Operation Franklin)* (compiler, YO Fortier), p. 427–48. Geological Survey of Canada, Ottawa, Memoir no. 320.
- Tennant JP, Mannion PD, Upchurch P, Sutton MD and Price GD** (2017) Biotic and environmental dynamics through the Late Jurassic–Early Cretaceous transition: evidence for protracted faunal and ecological turnover. *Biological Reviews* **92**, 776–814.
- Turner HE, Batenburg SJ, Gale AS and Gradstein FM** (2019) The Kimmeridge Clay Formation (Upper Jurassic–Lower Cretaceous) of the Norwegian Continental Shelf and Dorset, UK: a chemostratigraphic correlation. *Newsletters on Stratigraphy* **52**, 1–32.
- Tyson RV** (1995) *Sedimentary Organic Matter: Organic facies and playnofacies*. London: Chapman and Hall, 651 pp.
- Vickers ML, Price GD, Jerrett RM, Sutton P, Watkinson MP and FitzPatrick M** (2019) The duration and magnitude of Cretaceous cold events: Evidence from the northern high latitudes. *Geological Society of America (GSA) Bulletin* **131**, 1979–94.
- Vickers ML, Price GD, Jerrett RM and Watkinson M** (2016) Stratigraphic and geochemical expression of Barremian–Aptian global climate change in Arctic Svalbard. *Geosphere* **12**, 1594 doi: [10.1130/GES01344.1](https://doi.org/10.1130/GES01344.1)
- Voigt S and Hilbrecht H** (1997) Late Cretaceous carbon isotope stratigraphy in Europe: Correlation and relations with sea level and sediment stability. *Palaeogeography, Palaeoclimatology, Palaeoecology* **134**, 39–59.
- Weissert H and Channell JET** (1989) Tethyan carbonate carbon isotope stratigraphy across the Jurassic–Cretaceous boundary: an indicator of decelerated carbon cycling. *Paleoceanography* **4**, 483–94.
- Weissert H and Erba E** (2004) Volcanism, CO<sub>2</sub>, and palaeoclimate: A Late Jurassic–Early Cretaceous carbon and oxygen isotope record. *Journal of the Geological Society of London* **161**, 695–702.
- Weissert H and Mohr H** (1996) Late Jurassic climate and its impact on carbon cycling. *Palaeogeography, Palaeoclimatology, Palaeoecology* **122**, 27–43.
- Wierzbowski H and Joachimski M** (2009) Stable isotopes, elemental distribution, and growth rings of belemnoid belemnite rostra: proxies for belemnite life habitat. *Palaios* **24**, 377–86.
- Wimbledon WAP** (2017) Developments with fixing a Tithonian/Berriasian (J/K) boundary. *Volume Jurassica* **15**, 181–6.
- Wimbledon WAP, Casellato CE, Reháková D, Bulot LG, Erba E, Gardin S, Verreussel RMCH, Munsterman DK and Hunt CO** (2011) Fixing a basal Berriasian and Jurassic/Cretaceous (J/K) boundary - is there perhaps some light at the end of the tunnel? *Rivista Italiana di Paleontologia e Stratigrafia* **117**, 295–307.
- Wortmann UG and Weissert H** (2000) Tying platform drowning to perturbations of the global carbon cycle with a  $\delta^{13}\text{C}_{\text{org}}$ -curve from the Valanginian of DSDP Site 416. *Terra Nova* **12**, 289–94.
- Wright CW, Callomon JH and Howarth MK** (1996) Part L Mollusca 4 (revised) Cretaceous Ammonoidea Vol. 4. In *Treatise on Invertebrate Paleontology* (eds RL Kaesler *et al.*). Geological Society of America, Boulder and the University of Kansas, Lawrence.
- Yasuhara M, Ando A and Iba Y** (2017) Past emergent phase of Shatsky Rise deep marine igneous plateau. *Scientific Reports* **7**, 15423.
- Žák K, Košťák M, Man O, Zakharov VA, Rogov MA, Pruner P, Dzyuba OS, Rohovec J and Mazuch M** (2011) Comparison of carbonate C and O stable isotope records across the Jurassic/Cretaceous boundary in the Boreal and Tethyan Realms. *Palaeogeography, Palaeoclimatology, Palaeoecology* **299**, 83–96.
- Zakharov VA, Bogomolov Y, Il'ina VI, Konstantinov AG, Kurushin NI, Lebedeva NK, Meledina SV, Nikitenko BL, Sobolev ES and Shurygin BN** (1997) Boreal zonal standard and biostratigraphy of the Siberian Mesozoic. *Russian Geology and Geophysics* **38**, 965–93.
- Zakharov VA, Bown P and Rawson PF** (1996) The Berriasian stage and the Jurassic–Cretaceous boundary. In *Proceedings of the Second International Symposium on Cretaceous Stage Boundaries* (eds PF Rawson, AV Dhondt, JM Hancock and WJ Kennedy), p. 7–10. L'Institut Royal des Sciences Naturelles de Belgique, Brussels, Bulletin no. 66.
- Zakharov VA, Rogov MA, Dzyuba OS, Žák K, Košťák M, Pruner P, Skupien P, Chadima M, Mazuch M and Nikitenko BL** (2014) Palaeoenvironments and palaeoceanography changes across the Jurassic/Cretaceous boundary in the Arctic realm: case study of the Nordvik section (north Siberia, Russia). *Polar Research* **33**, 19714, doi: [10.3402/polar.v33.19714](https://doi.org/10.3402/polar.v33.19714)
- Ziegler PA** (1988) Evolution of the Arctic-North Atlantic and Western Tethys. *American Association of Petroleum Geologists Memoir* **43**, 198.